UNIVERSITY OF CALIFORNIA, SAN DIEGO

Towards Enzyme-directed Assembly of Micellar Nanoparticles

A thesis submitted in partial satisfaction of the requirements for the degree Masters of Science

in

Chemistry

by Steven Nguyen

Committee in Charge:

Professor Nathan Gianneschi, Chair
Professor Michael Burkart
Professor Cornelis Murre

2012

The Thesis of Steven Nguyen is approved, and it is acceptable in quality and form for publication on microfilm and electronically:

Chair

University of California, San Diego

2012

DEDICATION

This work is dedicated to those who thought it not possible to pursue a higher education in chemistry.

EPIGRAPH

Laudate Dominum.
Laudate Dominum.
Omnes! Gentes!
Alleluia!

TABLE OF CONTENTS

LIST OF ABBREVIATIONS

General:

μM	micromolar
μm	micrometer
μL	microliter
ACN	acetonitrile
ADEPT	antibody-directed enzyme prodrug therapy
7-ACA	7-aminocephalosporonic acid
BSA	bovine serum albumin
^{13}C NMR	carbon-13 nuclear magnetic resonance
CD_2Cl_2	deuterated dichloromethane
CALB	*Candida anartica lipase B*
COSY	^{1}H-^{1}H correlated spectroscopy
DABCYL	4,4 -Dimethylamino-azobenzene-4'-carboxylic acid
DCM	dichloromethane
DIPEA	N,N-diisopropylethylamine
DLS	dynamic light scattering
DMF	dimethylformamide
DMF-d_7	deuterated dimethylformamide
DMSO	dimethyl sulfoxide
DNA	deoxyribonucleic acid
ECM	extracellular matrix
EDANS	5-((2-Aminoethyl)amino)naphthalene-1-sulfonic acid
EDAPT	enzyme-directed assembly of particle theranostics
EPR	enhanced permeability and retention
ES-MS	electrospray mass spectrometry
EtOAc	ethyl acetate
FRET	fluorescence resonance energy transfer
g	grams
^{1}H NMR	proton nuclear magnetic resonance
H_2O	water
H_3PO_4	phosphoric acid
HCl	hydrochloric acid
HPLC	high performance liquid chromatography
HR-MS	high resolution mass spectrometry
Hz	Hertz
LiBr	lithium bromide
M	molar
MeOH	methanol
mg	milligrams
$MgCl_2$	magnesium chloride
min	minutes
mL	milliliters

mmol	millimoles
MMP	matrix metalloproteinase
M_n	number average molecular weight
MT1-MMP	membrane type 1 metalloproteinase
Mz	average molecular weight
m/z	mass per unit charge
N	normal
$NaHCO_3$	sodium bicarbonate
nM	nanomolar
NMR	nuclear magnetic resonance spectroscopy
PBS	phosphate-buffered saline
PDI	polydispersity index
PDEPT	polymer-directed enzyme prodrug therapy
PEG	polyethylene glycol
ppm	parts per million
R_f	retention factor
ROMP	ring-opening metathesis polymerization
SLS	static light scattering
TEA	triethylamine
TEM	transmission electron microscopy
TFA	trifluoroacetic acid
THF	tetrahydrofurane
TLC	thin layer chromatography
Tris•HCl	tris(hydroxymethyl)aminomethane hydrochloric acid

For nuclear magnetic resonance spectroscopy:

δ	nuclear magnetic resonance chemical shift in ppm
bs	broad singlet
d	doublet
dd	doublet of doublet
m	multiplet
s	singlet
t	triplet

LIST OF FIGURES

LIST OF TABLES

ABSTRACT OF THE THESIS

Towards Enzyme-directed Assembly of Micellar Nanoparticles

by

Steven Nguyen

Master of Science in Chemistry

University of California, San Diego 2012

Professor Nathan Gianneschi, Chair

In recent years, there have been significant strides towards the development of nanomaterials for biomedical applications with a particular focus on selective targeting and cytotoxic drug delivery. However, there is a recognized need for the development of new and advanced strategies towards improved targeting and endosome escape. Herein, we present stimuli-responsive polymeric materials capable of undergoing well-defined and enzyme-directed assembly and/or release of cargo. These systems aim to address a key issue concerning drug-delivery systems, namely the selective and specific targeting of diseased cells and avoidance of non-specific side-effects. β-lactamase-responsive,

doxorubicin-labeled, and peptide substrates were synthesized towards generating enzymatically responsive materials capable of providing an alternative and improved approach for the localization and visualization of drug delivery processes mediated by cell-membrane proteases associated with metastatic cancer. These functionalized materials may eventually serve as molecular diagnostics for disease detection and drug release.

doxorubicin-labeled, and peptide substrates were synthesized towards generating enzymatically responsive materials capable of providing an alternative and improved approach for the localization and visualization of drug delivery processes mediated by cell-membrane proteases associated with metastatic cancer. These functionalized materials may eventually serve as molecular diagnostics for disease detection and drug release.

Chapter 1 – Introduction

1.1 – General Overview

The focus of this thesis is the development of nanomaterials that are capable of interacting with and responding to specific enzymatic biochemical signals associated with specific disease states, tissues, and pathogens. The preparation of multifunctional nanoscale materials requires advanced synthetic methods and techniques. Therefore towards these materials, our goals are two-fold. We aim 1) to develop methods for the preparation and synthesis of well-defined programmable nanomaterials and 2) to utilize enzymatic action on dynamic materials as a diagnostic and drug delivery mechanism. Herein, we present two strategies towards the development of enzyme-responsive materials; 1) The development of materials that are responsive to metalloproteases associated with metastatic cancer and 2) The development of a material that responds to non-eukaryotic bacterial enzymes with utility in prodrug activation and delivery strategies. The general design of these enzyme-responsive materials capable of forming specific nanostructures with specific spectrophotometric properties is shown in **Figure 1.1**. Furthermore, **Figure 1.1** illustrates the general design of brush polymers capable of behaving as macro-prodrugs. Ultimately, these materials are designed for the purpose of drug targeting and endosomal release.

Our design strategy is inspired by antibody-directed enzyme prodrug therapy (ADEPT) and polymer-directed enzyme prodrug therapy (PDEPT) shown in **Figure 1.1A & B**. These are both methods that provide attractive approaches to selective targeted drug delivery. Both approaches rely on a strategy to guide enzymes to a specific site *in vivo*, in

which the enzyme activates prodrugs in order to inhibit tumor growth.[1-9] These methods have shown promise but have not been fully realized in the treatment of cancer and disease associated tissues. Indeed, neither approach has proven to be very effective in clinical applications. Such downfalls are a result of the clearance of prodrug relative to the inherent slow pharmacokinetics of antibodies and the relatively low enzyme concentration achieved in contrast to prodrug delivery.[10] With significant room for improvement, these methods have inspired us to develop new materials capable of accumulating at targeted sites and systems for single step delivery of targeting group, drug and enzyme.

In targeting cancer cells, matrix metalloproteinases (MMPs) are potentially excellent biomarkers.[11-14] MMP-2 and MMP-9 are the most well characterized proteases in this respect, which are secreted in the extracellular matrix (ECM) or are membrane bound as for membrane type 1-matrix metalloproteinase (MT1-MMP).[15,16] Therefore, a step towards targeted drug delivery is the proteolytic cleavage of MT1-MMP peptide substrates at metastatic cell membranes.[12] **Figure 1.1C** demonstrates the cleavage of such substrates that may provide a diagnostic tool for the detection of diseased tissues. This approach would exploit the catalytic turnover of endogenously expressed MT1-MMP enzymes. Furthermore, MT1-MMPs are cycled into endosomes rapidly in a cyclical fashion and is associated with integrins when at the cell surface.[17-19] We hypothesized that polymeric nanomaterials specifically targeted to integrin receptors and responsive to MT1-MMPs, would localize near the protease and be internalized via endosomal uptake for activated cleavage and endosomal release as illustrated in **Figure 1.1E**. It is important to note that an approach utilizing enzymes to amplify release from endosomes has not

been demonstrated in practice. Therefore, in Chapter 1 we will describe the synthesis and approach towards disease-associated peptide substrates responsive to MT1-MMP.

In addition to the development of systems capable of activating in response to endogenous enzymes, we seek to combine targeting, exogenously added enzyme, and prodrug for the controlled, specific, and selective delivery of drugs. **Figure 1.1D** proposes a strategy that entails an enzyme-responsive prodrug polymer containing a targeting group and an enzyme that is purposely inactive. Inactivating the enzyme prevents the premature cleavage of the cytotoxic drug at unwanted sites. However, when the targeting group is bound to the diseased cell, the inhibited enzyme can be activated by MMPs. The prodrug polymer conjugate enzyme is then able to hydrolyze the prodrug when uninhibited. This method allows for the localization to diseased tissues and controlled prodrug release. In an attractive strategy, we aim to transfect cancer cells with the genetic code for a bacterial enzyme, allowing the expression and localization of activating enzyme at the tumor site demonstrated in **Figure 1.1F**. By introducing the enzyme-responsive material developed in this thesis, the prodrug can then only be activated and cleaved at the site of bacterial enzyme expression. However, the transfection of cancer cells and design for inhibiting a prodrug-activating enzyme are not our main focus here but rather, we aim to develop materials capable of enzyme-directed assembly, destruction and/or prodrug release for eventual implementation of these potential strategies.

Figure 1.1: Strategies for enzyme prodrug therapy. A) ADEPT. (i) Antibody circulates the vasculature. (ii) Antibody binds to cell surface antigen of a tumor cell. (iii) Prodrug polymer conjugate or standard small molecule pro-drug is introduced and cleaved by the enzyme covalently linked to the antibody. B) PDEPT. (i) Prodrug polymer conjugate accumulates at tumor site via the EPR effect. (ii) Activating enzyme polymer is introduced into the vasculature. (iii) Prodrugs are released by the activating enzyme. C) MMP cleavage. (i) Prodrug substrate polymer is recognized by either MT1-MMP at the cell surface or MMPs secreted in the ECM. (ii) Prodrug polymer is cleaved by MMPs to release the drug. D) Targeted prodrug inactive enzyme polymer. (i) Antibody binds to cancer cell. (ii) Tumor associated protease activates enzyme polymer. (iii) Prodrugs are cleaved by the attached active enzyme. E) Enzyme-driven and release. (i) Targeting group of the prodrug polymer binds to integrin at the cell surface. (ii) Targeted prodrug polymer is engulfed. (iii) Targeted prodrug polymer is inside the endosome. (iv) Prodrug is cleaved by the membrane-anchored protease. (v) Drugs are release into the cytosol via endosomal escape. F) Trasnfection enzyme prodrug therapy. (i) Cancer cells are transfected with foreign DNA for the expression of a bacterial enzyme. (ii) Bacterial enzyme is expressed and excreted to the ECM. (iii) Prodrug polymer conjugate is introduced. (iv) Prodrug polymer conjugate is cleaved by the enzyme. G) Key for corresponding figures.

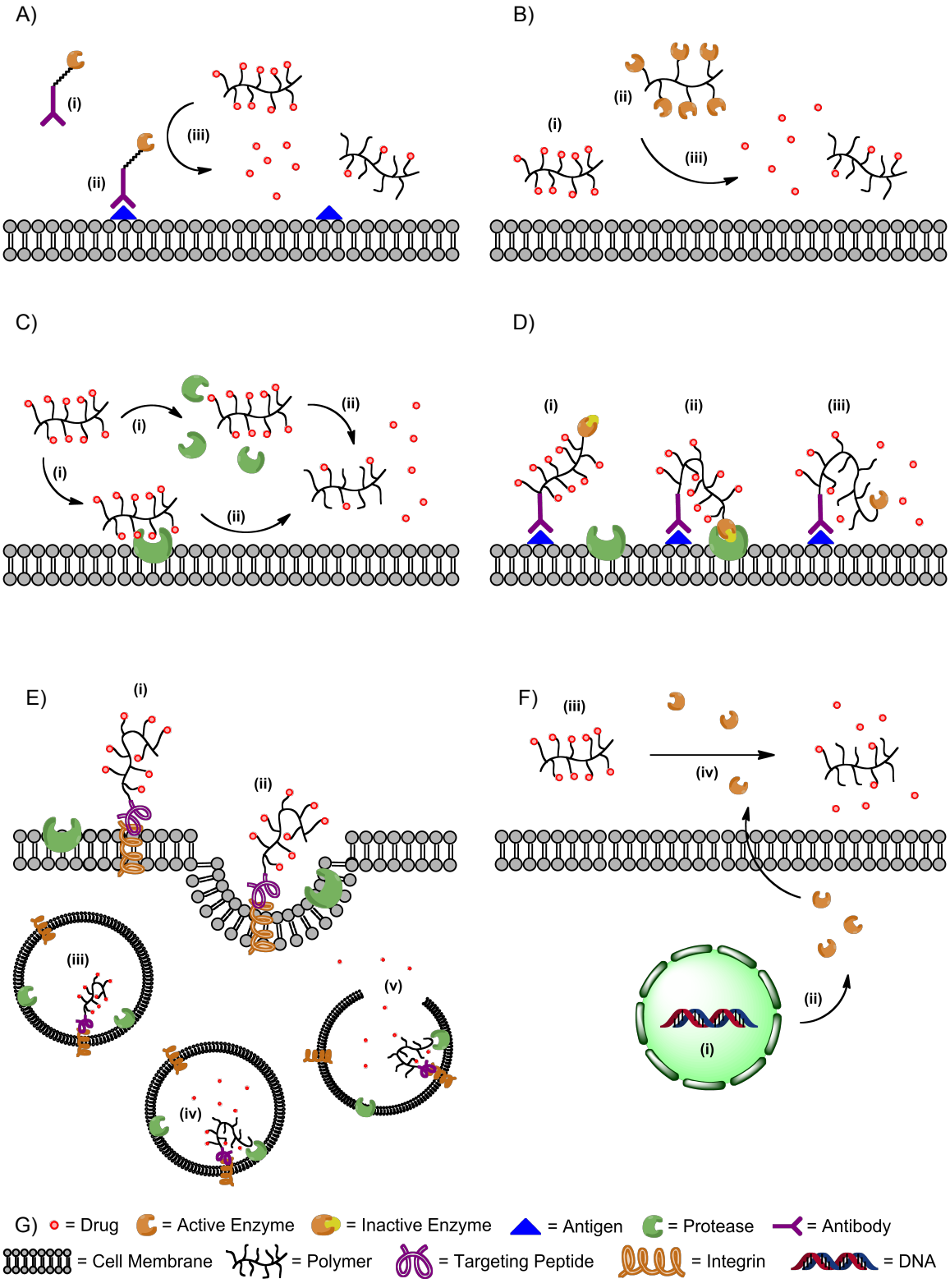
A)
(i)
(ii)
(iii)
B)
(i)
(ii)
(iii)
C)
(i)
(ii)
(i)
(ii)
D)
(i)
(ii)
(iii)
E)
(i)
(ii)
(iii)
(iv)
(v)
F)
(iii)
(iv)
(i)
(ii)
G)
= Drug
= Active Enzyme
= Inactive Enzyme
= Antigen
= Protease
= Antibody
= Cell Membrane
= Polymer
= Targeting Peptide
= Integrin
= DNA

The key concept towards enzyme prodrug therapy is designing a material that can be exclusively cleaved by a specific activating enzyme and not by various non-specific endogenously expressed enzymes. The enzyme must be bioorthogonal in humans for each of the methods described, hence the utilization of foreign enzymes in delivery strategies such as ADEPT and PDEPT. Specifically, β-lactamase has been utilized in both ADEPT and PDEPT, which has orthogonal activity within mammalian systems.[3,9,20] However, the use of β-lactamase presents a concern because this enzyme may cause an immunological response. We note, this may be mitigated by the use of targeted humanized enzymes in future manifestation of the approach.[5]

With each of these strategies, materials containing prodrugs can be activated and released as potential therapeutics. Furthermore, the incorporation of dyes within these materials could serve as a marker for the detection of cancer cells in response to enzyme activity.[11] However, these methods alone are not sufficient towards such advances. Overall, we are interested in the enzyme-directed assembly of micellar nanoparticles. This approach harnesses both the incorporation of dyes and the release of drug as a molecular diagnostic tool and a strategy for prodrug therapy. The formation of nanoscale micelles and larger species can serve as an amplification signal for selective enzyme activity and disease detection as these materials accumulate *in situ* and not do wash away (patent pending).[21,22] We term this strategy enzyme-directed assembly of particle theranostics (EDAPT). Herein we develop an approach utilizing β-lactamase and MT1-MMP as activators for the formation of micellar nanoparticles and the release of small molecules.

1.2 – Background of Enzyme Prodrug Therapies

In the treatment of cancer, there is a recognized need for advanced methods in targeting drug delivery and diagnostic. Antibody-directed enzyme prodrug therapy (ADEPT) has provided a selective approach towards cell targeting and delivery of such anticancer agents to the tumor site.[1-5,10] This two-step approach relies on antibody recognition of cancer-associated antigens followed by the catalytic activity of a covalently linked enzyme to cleave anticancer drugs from a prodrug polymer. In theory, the advantage of antibody localization allows for the selective and specific recognition of cancer cells avoiding toxicity to normal tissues. A related approach has been proposed using PDEPT. Similarly PDEPT is a two-step method in which the enhanced permeability and retention (EPR) effect is responsible for the extra vasculature accumulation of polymeric prodrug at the tumor.[4,7,8] Chased by a corresponding polymer-enzyme conjugate, the enzyme activity should be capable of liberating the cytotoxic drug at the accumulation site. However, each of these approaches suffer from the inability to accumulate sufficient concentrations of drug.[10] Our approach involves the assembly of nano- and microparticles within tumor tissue in response to enzymes. This has the effect of accumulating material within tumors while allowing clearance from the circulation, creating a beneficial difference in targeted vs non-targeted materials. We term this approach, EDAPT (as noted in the previous section). This approach can utilize either endogenous enzymes (patent pending),[5] or could possibly be adapted for responding to targeted, exogenously added enzymes as in ADEPT.

Towards these methods, cephalosporin-based prodrug substrates have been synthesized and integrated within these prodrug therapies.[3,8,9,20] In this manner, β-

lactamase catalytic activity has shown suppression of tumor growth.[3,6,9,20] Cephalosporin-based prodrugs are beneficial in selective prodrug hydrolysis because endogenous enzymes cannot activate these substrates. The use of β-lactamase allows for the non-cytotoxicity of normal cells and the suppression of targeted tumors. Thus the essential benefits of β-lactamase in the activation and delivery of prodrugs has encouraged the development for new strategies described in this thesis.

1.3 – Background of Metalloproteases For Targeting Probes

In the development of cancer, MMPs are overexpressed at the cell surface and the ECM.[12,15,23,24] MMPs, either membrane anchored or excreted, are zinc-dependent proteolytic peptidases that degrade the ECM and cleave various cell surface receptors. MMP-2 and MMP-9 are the most overexpressed proteases associated with tumors.[15,23] These zymogens are activated by MT1-MMP catalytic activity. The proteolytic activation of peptide substrates has been proven as a means for the localization of probes and detection of cancers.[11,12] Additionally, MT1-MMP has also been demonstrated as a FRET biosensor for the visualization of protease expression.[11,12] These expression patterns provide the basis for developing and designing nanomaterial containing peptide substrates for the targeting of cancer. In this thesis, we describe the design of a dye-labeled peptide substrate monomer towards the targeting of diseased state tissues overexpressing MT1-MMP.

1.4 – Efforts to Develop Enzyme-Responsive and Enzyme-Assembled Organic Materials

The development of various molecular systems within functionalized nanomaterials has directed an increasing interest of polymeric biomaterials towards biomedical and material science applications. Significant contributions have been made towards the synthesis and design of polymers suitable for programmed and controlled manipulation of these materials. The development of smart polymers has thus enabled the introduction of stimuli-responsive polymers sensitive to solvent, pH, temperature, light, enzymes, and various stimuli.[25-28] The intrinsic properties of these functionalized materials provide methods for the assembly, disassembly, and morphological changes of various polymeric materials into functionalized nanostructures.[21,29,30] The activation of stimuli-responsive polymers further allows the capability of undergoing morphological changes from polymer to micelle to cylinders to lamellar structures and other nanostructures as illustrated in **Figure 1.2**.[21,22,31] Remarkably, despite numerous stimuli having been explored in the supramolecular assembly of nanomaterials, there has been little work on the assembly of micellar nanoparticles utilizing enzymes.

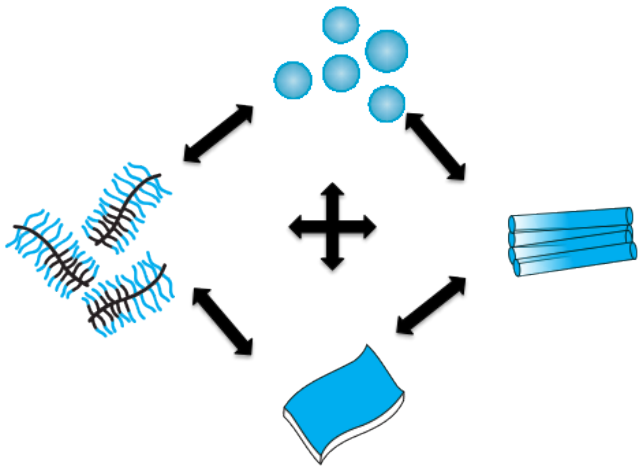

Figure 1.2: Morphological switches and phase changes of polymeric materials.

Recently, the self-assembly of enzymatically triggered block copolymers has been shown using a pre-amphiphilic block copolymer.[28] Hydrophilic moieties installed in the pre-amphiphilic polymer design allows for full water solubility, in which the soon-to-be hydrophobic block is decorated with phosphates. Upon dephosphorylation via a phosphatase, the hydrophobic region is exposed, changing the properties of the polymer. The activated pre-amphiphile now behaves as an amphiphile and consequently self-assembles into micellar nanoparticles. This previous example using a phosphatase as the activating enzyme has inspired us to incorporate more specific and less general enzymes, amendable to true biotic conditions. Herein, we describe the design of cephalosporin-based polymers and MT1-MMP substrate-linked polymers that are selectively cleaved by β-lactamase and proteases for the self-assembly of micellar nanoparticles and prodrug activation.

1.5 – References

(1) Bagshawe, K. D.; Napier, M. *Enzyme-Prodrug Strategies for Cancer Therapy* **1999**, 199-207.

(2) Bagshawe, K. D.; Sharma, S. K.; Springer, C. J.; Rogers, G. T. *Ann Oncol FIELD Full Journal Title:Annals of oncology : official journal of the European Society for Medical Oncology / ESMO* **1994**, *5*, 879-91.

(3) Blau, L.; Menegon, R. F.; Chung, M. C. *Quimica Nova* **2006**, *29*, 1307-1317.

(4) Satchi, R.; Connors, T. A.; Duncan, R. *British Journal of Cancer* **2001**, *85*, 1070-1076.

(5) Smith, G. K.; Banks, S.; Blumenkopf, T. A.; Cory, M.; Humphreys, J.; Laethem, R. M.; Miller, J.; Moxham, C. P.; Mullin, R.; Ray, P. H.; Walton, L. M.; Wolfe, L. A., III *Journal of Biological Chemistry* **1997**, *272*, 15804-15816.

(6) Duncan, R.; Gac-Breton, S.; Keane, R.; Musila, R.; Sat, Y. N.; Satchi, R.; Searle, F. *Journal of Controlled Release* **2001**, *74*, 135-146.

(7) Satchi, R.; Connors, T. A.; Duncan, R. *Proceedings of the International Symposium on Controlled Release of Bioactive Materials* **1999**, *26th*, 126-127.

(8) Satchi, R.; Duncan, R. *Proceedings of the International Symposium on Controlled Release of Bioactive Materials* **1997**, *24th*, 773-774.

(9) Satchi-Fainaro, R.; Hailu, H.; Davies, J. W.; Summerford, C.; Duncan, R. *Bioconjugate Chemistry* **2003**, *14*, 797-804.

(10) Springer, C. J.; Poon, G. K.; Sharma, S. K.; Bagshawe, K. D. *Cell Biophysics* **1994**, *24/25*, 193-207.

(11) Ouyang, M.; Huang, H.; Shaner, N. C.; Remacle, A. G.; Shiryaev, S. A.; Strongin, A. Y.; Tsien, R. Y.; Wang, Y. *Cancer Res* **2010**, *70*, 2204-12.

(12) Jiang, T.; Olson, E. S.; Nguyen, Q. T.; Roy, M.; Jennings, P. A.; Tsien, R. Y. *Proc Natl Acad Sci U S A* **2004**, *101*, 17867-72.

(13) Liu, S.; Netzel-Arnett, S.; Birkedal-Hansen, H.; Leppla, S. H. *Cancer Research* **2000**, *60*, 6061-6067.

(14) Scherer, R. L.; McIntyre, J. O.; Matrisian, L. M. *Cancer Metastasis Rev* **2008**, *27*, 679-90.

(15) Lombard, C.; Saulnier, J.; Wallach, J. *Biochimie FIELD Full Journal Title:Biochimie* **2005**, *87*, 265-72.

(16) Maatta, M.; Soini, Y.; Liakka, A.; Autio-Harmainen, H. *Am J Clin Pathol* **2000**, *114*, 402-11.

(17) Bachmann, A. S.; Surovoy, A.; Jung, G.; Moelling, K. *Journal of Molecular Medicine (Berlin)* **1998**, *76*, 126-132.

(18) Curley, G. P.; Blum, H.; Humphries, M. J. *Cellular and Molecular Life Sciences* **1999**, *56*, 427-441.

(19) Burkhart, D. J.; Kalet, B. T.; Coleman, M. P.; Post, G. C.; Koch, T. H. *Molecular Cancer Therapeutics* **2004**, *3*, 1593-1604.

(20) Vrudhula, V. M.; Svensson, H. P.; Senter, P. D. *Journal of Medicinal Chemistry* **1995**, *38*, 1380-5.

(21) Chien, M. P.; Rush, A.; Thompson, M.; Gianneschi, N. *Angewandte Chemie International Edition* **2010**, *49*, 5076-5080.

(22) Ku, T. H.; Chien, M. P.; Thompson, M. P.; Sinkovits, R. S.; Olson, N. H.; Baker, T. S.; Gianneschi, N. C. *J Am Chem Soc* **2011**, *133*, 8392-5.

(23) Kessenbrock, K.; Plaks, V.; Werb, Z. *Cell* **2010**, *141*, 52-67.

(24) Maatta, M.; Santala, M.; Soini, Y.; Turpeenniemi-Hujanen, T.; Talvensaari-Mattila, A. *Acta Obstet Gynecol Scand* **2010**, *89*, 380-4.

(25) Dreher, M. R.; Simnick, A. J.; Fischer, K.; Smith, R. J.; Patel, A.; Schmidt, M.; Chilkoti, A. *J Am Chem Soc FIELD Full Journal Title:Journal of the American Chemical Society* **2008**, *130*, 687-694.

(26) Lee, S. C.; Lee, H. J. *Langmuir* **2007**, *23*, 488-95.

(27) Lee, H. i.; Wu, W.; Oh, J.; Mueller, L.; Sherwood, G.; Peteanu, L.; Kowalewski, T.; Matyjaszewski, K. *Angewandte Chemie International Edition* **2007**, *46*, 2453-2457.

(28) Amir, R. J.; Zhong, S.; Pochan, D. J.; Hawker, C. J. *Journal of the American Chemical Society* **2009**, *131*, 13949-13951.

(29) Agut, W.; Brulet, A.; Schatz, C.; Taton, D.; Lecommandoux, S. *Langmuir* **2010**, *26*, 10546-10554.

(30) Chen, Y.; Dong, C.-M. *The Journal of Physical Chemistry B* **2010**, *114*, 7461-7468.

(31) Chien, M.-P.; Gianneschi, N. C.; (University of California, USA). Application: WO, 2011, p 168pp.

Chapter 2: Synthesis of Stimuli-Responsive Monomers

2.1 – Introduction

Towards the synthesis of enzyme-responsive materials, we specifically aimed to design monomers containing moieties that are capable of being delivered by enzymes associated with cancer cells and/or bacterial enzymes. We hypothesized that exploiting β-lactamase and MT1-MMP enzymes would allow the selective and controlled response of these polymeric systems towards such purposes.[1-4] To generate stimuli-responsive materials, a library of monomers that are highly functionalized had to be synthesized. These monomers are functionalized with norbornene to install olefins that allow polymerization of these monomers. To elicit a response, these monomers each contain a stimuli-responsive linker; either enzymatic or pH triggered. Moreover, these monomers also contain a leaving group such as a drug, dye, hydrophilic moiety, or small molecule for the targeted cleavage of these polymeric materials. By designing monomers that contain a polymerizable group, stimuli-responsive linker, and targeting group, a multitude of highly functionalized monomers can be generated to develop novel methods for micelle assembly, disease detection and prodrug activation as illustrated in **Figure 2.1**. Herein, we describe the synthesis of stimuli-responsive monomers **1-4**.

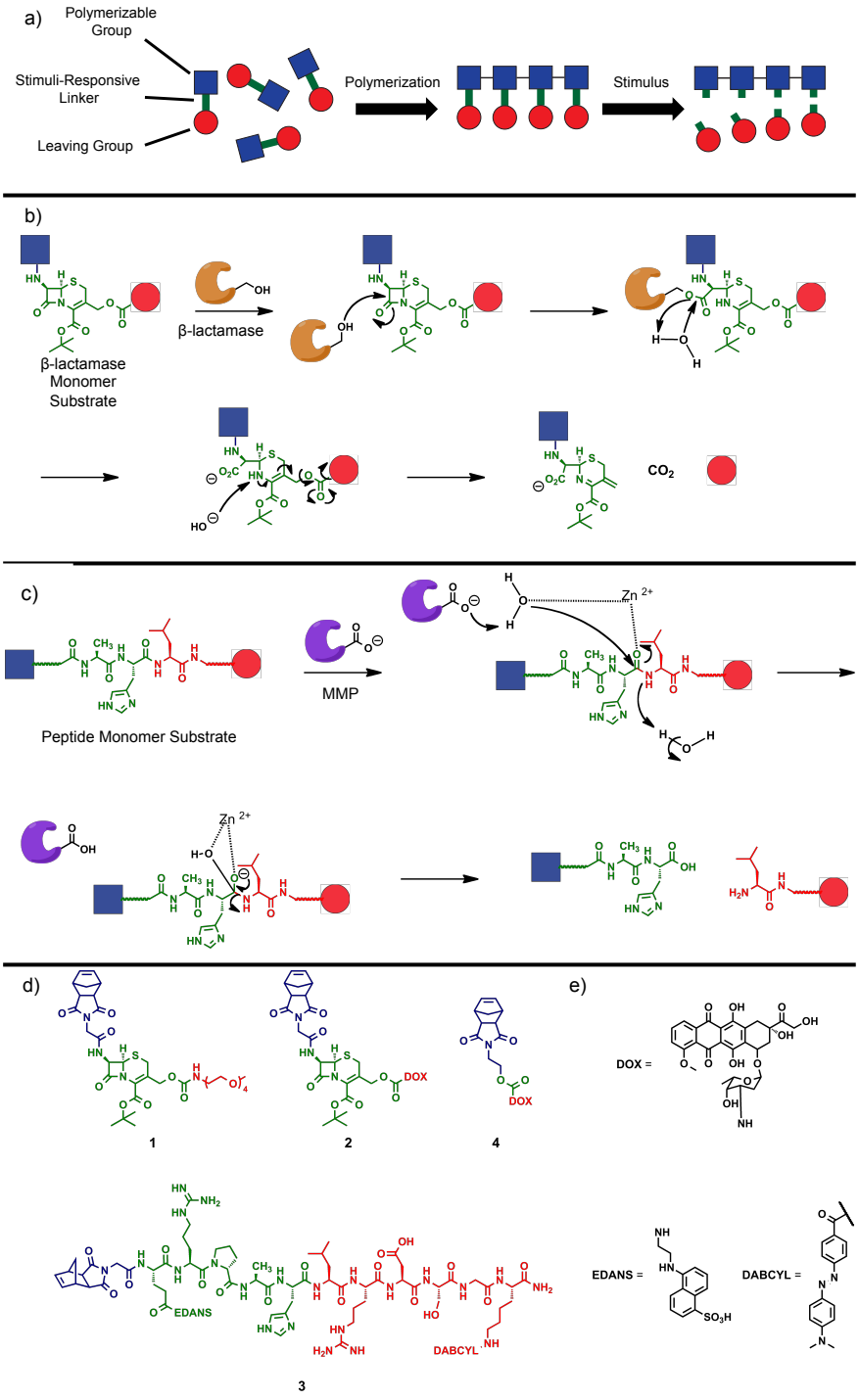

Figure 2.1: Design of stimuli-responsive monomers. a) Monomer design and activation of stimuli-responsive polymers. b) Mechanism of β-lactamase. c) Mechanism of MMP.

d) Structure of monomers **1-4**. e) Structures of substituted abbreviations. Blue: Polymerizable group. Green: Stimuli-responsive linker. Red: Leaving group.

2.2 – Synthesis of β-lactamase-Responsive Monomers

Enzymes have been surprisingly underutilized in regards to the discrete assembly of organic nanoparticles. The first report to be published demonstrates the abiotic enzymatically triggered self-assembly of block copolymers to generate micelles.[5] While an excellent proof-principle, these materials respond via a dephosphorylation catalyzed by a general phosphatase and are therefore non-selective and difficult to couple with specific biochemical signals. Therefore, there is significant room for advancement towards enzyme-directed material assembly.

Taking advantage of its foreign nature within eukaryotes, β-lactamase serves as a good first choice for controlled and specific prodrug activation by an exogenous enzyme. Herein, we aimed to prepare cephalosporin-based monomers. In this chapter, the synthesis of β-lactamase-responsive monomers **1** & **2** are described.

2.2.1 – Cephalosporin-Based Monomer Synthesis

7-aminocephalosporonic acid (7-ACA) contains many functional groups that must be taken into consideration during synthetic manipulation. Three main functional groups that allow for synthetic modification are the free 7'-amino group, acetyl protected alcohol at the 3'-end, and the free carboxylic acid as demonstrated in **Figure 2.2**. In addition to functional group complexity, conjugation, protection, and deprotection at these sites allow for the synthesis of enzyme-responsive monomers.

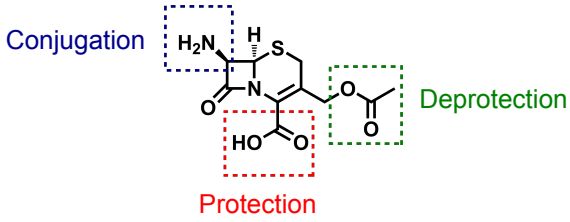

Figure 2.2: Functional group modifications of 7-ACA.

In the synthesis of cephalosporin-based monomers, an initial drawback is the lack of general solubility of 7-ACA in common organic solvents. To address this issue, solvent conditions were adjusted by adding triethylamine (TEA), a non-nucleophilic base, to the solution containing the material. We soon realized that in the presence of base, 7-ACA would dissolve in several organic solvents including dimethylformamide (DMF) and acetonitrile (ACN). For this reason, we carried out our initial reactions using both solvents.

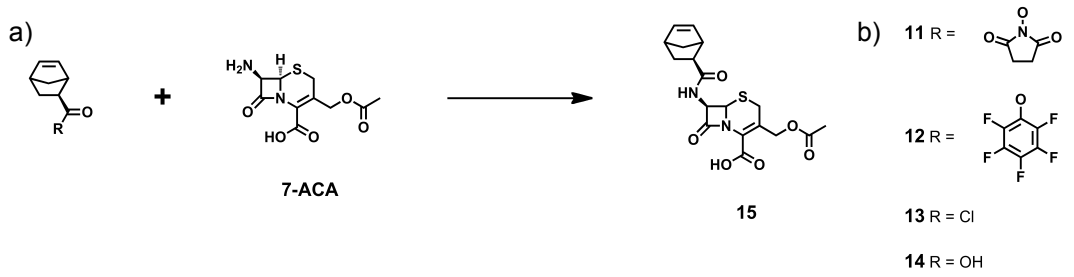

Figure 2.3: Conjugation strategies for installing the polymerizable group on 7-ACA. a) Synthesis of compound **15**. b) R groups of compounds **11**, **12**, **13** & **14**.

Circumventing the solubility issue, attempts to conjugate 7-ACA to a norbornene unit serving as the polymerizable group to afford **15** were carried out using various

compounds. The attempted conjugation reactions are shown in **Figure 2.3**. Dissymmetric norbornene compound **11**, containing a N-hydrosuccinimide activated ester was first used. However, after many unsuccessful attempts, pentafluorophenol norbornene ester **12** was used instead as the conjugatable compound. With the failure of both norbornene-activated esters, dissymmetric acyl chloride **13** was synthesized from compound **14** in hopes of 7-ACA conjugation to obtain **15**. Despite the many efforts, the synthesis of compound **15** remained unsuccessful through the use of compounds **11-13**. With the many unsuccessful attempts, we abandoned the dissymmetric norbornene and switched to **5**. Compound **5** was chosen because of the symmetry that exists within the molecule. The symmetrical nature of **5** results in a greatly simplified ^{1}H NMR spectrum that allow for the ease of assignment and minimizes peak overlap in the monomers described. Moreover, compound **5** contains a glycine spacer between norbornene and the cephalosporin linker. We rationalized that this would provide flexibility within the polymer due to the spacer and therefore, greater accessibility to the enzyme. For these reasons, we abandoned compound **11-13** and focused on compound **5**.

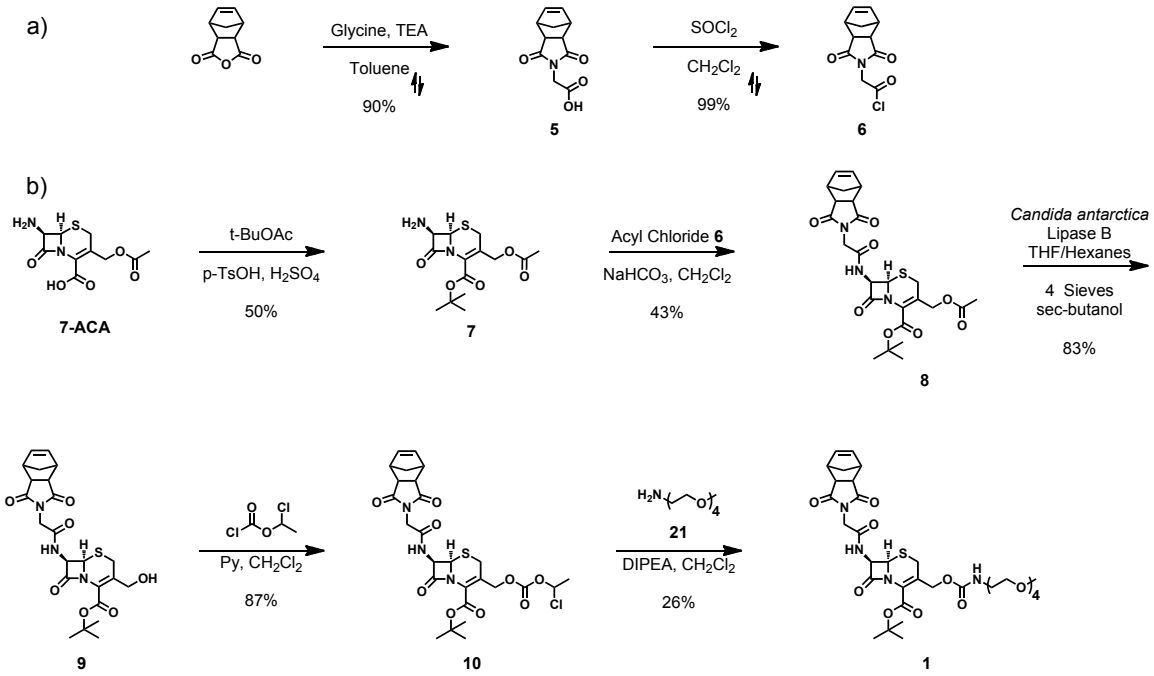

Figure 2.4: Synthesis of cephalosporin-based monomers. a) Synthesis of acyl chloride **6**. b) Synthesis of monomer **1**.

After experiencing solubility issues, we averted our attention towards the protection of the free carboxylic acid rather than conjugation at the 7' amine for the synthesis of compound **7**. The carboxylic acid was *tert*-butyl protected using *tert*-butyl acetate, *p*-Toluene sulfonic acid, and sulfuric acid as reagents. 7-ACA was not originally soluble in the reaction mixture, however over a period of time, a majority of the suspension dissolved in solution. In the previous case of using base to solubilize 7-ACA, protonating with acid drives the material to solubilize which is the reason for the presence of *p*-Toluene sulfonic acid and sulfuric acid. The presence of base or acid assists in introducing polarity within the molecule to solubilize in selective organic solvents. After purification, we typically observed approximately 50% yield of **7**, which may be

accounted for by the lack of full solubility of 7-ACA. Despite the percent yield, solubility no longer remains an issue for product **7** as the material fully dissolves in organic solvent. As compound **7** readily dissolves, the amine can now be conjugated to compound **6** with ease. In the preparation of compound **6**, the reaction must be air free as the acyl chloride product is sensitive to moisture. In the presence of moisture, compound **6** can easily be hydrolyzed to generate compound **5**. Thus in conjugating small molecules to **6**, the material is freshly made before reaction and the solvent is evacuated on the Schlenk line using a secondary trap. This technique eliminates exposure of **6** to moisture before being added to the reaction.

In the synthesis of compound **8**, compound **6** was pre-dissolved in dry dicholoromethane (DCM) and transferred under pressurized nitrogen via cannula into the cooled vigorously stirring reaction mixture containing compound **7**. The DCM and saturated sodium bicarbonate ($NaHCO_3$) solution reaction mixture presents many concerns, chiefly the presence of aqueous solvent. The water present in the mixture accounts for the low yield in which compound **6** is hydrolyzed. Thus to maximize product yield, the reaction mixture was cooled to allow the nucleophilic strength of the amine to attack the acyl chloride as well as to delay hydrolysis. We optimized by adding **6** in excess to account for the unwanted hydrolysis. Although the reaction conditions are adjusted to increase the yield of compound **8**, less than 50% yield is observed. Despite the hydrolysis of **6**, compound **5** can be recovered by acidifying the saturated $NaHCO_3$ solution with concentrated hydrochloric acid (HCl) and extracted with DCM. Even though excess acyl chloride is used for the synthesis of **8**, the recovery of **5** can be used to resynthesize compound **6**.

With the protected carboxylic acid, the 3'-alcohol can now be de-acetylated to obtain compound **9**. Deprotection of the alcohol can be carried out using either acid/base hydrolysis or lipase enzymes. Regardless of whether the carboxylic acid is protected or not, using either acid or base will allow the formation of a deleterious 5-membered lactone ring as illustrated in **Figure 2.5**.[6] Both esters are initially hydrolyzed permitting the cyclization of the lactone. Thus we turned to lipase as the means to selectively deprotect the alcohol. Because compound **8** contains two esters, the deprotection must be selective for the alcohol and not the carboxylic acid. To circumvent this problem, we used *Candida antartica Lipase B* (CALB*)* which is specific for the de-acetylation of the 3'-alcohol. CALB is also preferred over other lipase enzymes because it does not allow the formation of the isomerized product of the 4' olefin.[6] Using CALB, we were able to avoid the lactone side product and obtain relatively high yield of 85% of compound **9**

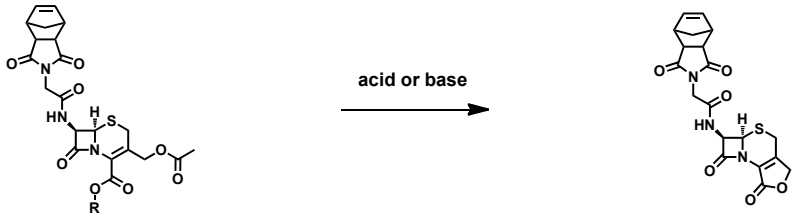

Figure 2.5: Synthesis of unwanted lactone product.

Obtaining compound **9** allows for the free hydroxyl group to conjugate to various small molecules such as a dye, drug, or polyethylene glycol (PEG). **Figure 2.6** demonstrates the attempts towards attaching the hydroxyl group of **9** directly to compound **20** through the use of various bases. However, the synthesis of compound **22** was unsuccessful. We believe that compound **9** is not a strong nucleophile, thus we

adjusted the synthesis by incorporating an extremely reactive electrophile that would drive the reaction for an addition-elimination nucleophilic attack. 1-Chloroethyl chloroformate was used as the carbonate linker in which, the acyl chloride is prone to nucleophilic attack by compound **9** to afford compound **10**.

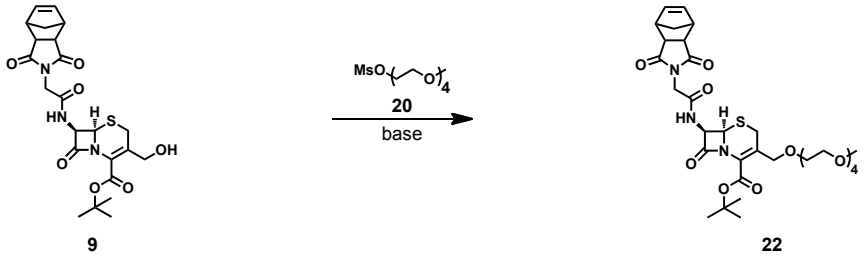

Figure 2.6: Attempted synthesis of compound **25**.

Incorporating the chloroformate introduces a new functionality into compound **10**, in which the presence of an activated carbonate ester allows a nucleophilic small molecule to attach at the electrophilic center. Towards the synthesis of **1**, the amine from compound **21** was directly attached to the activated carbonate ester to allow the more stable carbamate linkage. In the purification process, minor problems arose when running flash chromatography on silica gel due to poor separation. We ran a short plug of a silica column to recover compound **9**, with excess **21** and product immobile at the baseline. After collecting **9**, the column was eluted with 8.5:1:0.5 methanol (MeOH)/DCM/ethyl acetate (EtOAc). Two spots ran close on the column and separation was difficult. To purify monomer **1**, the material was further purified by high performance liquid chromatography (HPLC) and lyophilized to afford 26% yield.

In summary, monomer **1** could be prepared in 7 steps in a total yield of 3.6%. The reactions described should be optimized to obtain an overall higher yield. Despite the low yield, we have shown that 400-500 mg of **1** have been prepared. Through this multi-step synthesis, we have also synthesized compound **10** which can be drug labeled as described in the next section. Here we validated the synthesis of monomer **1** and its cephalosporin analogs towards the development of β-lactamase-responsive monomers.

2.2.2 –Doxorubicin-linked Cephalosporin Monomer Synthesis

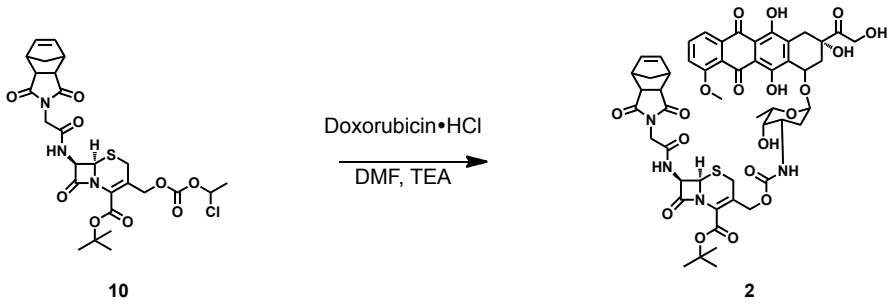

Figure 2.7: Synthesis of monomer **2**.

Doxorubicin•HCl was conjugated to compound **10** to afford β-lactamase-responsive prodrug monomer **2** demonstrated in **Figure 2.7**. The activated carbonate ester in compound **10** was susceptible to a nucleophilic attack via the amine of doxorubicin•HCl to form the carbamate-linked prodrug. Monomer **2** was characterized by proton nuclear magnetic resonance (^{1}H NMR) and confirmed by high-resolution mass spectrometry (HRMS). By conjugating doxorubicin to compound **10**, we were able to

synthesize a prodrug monomer capable of β-lactamase hydrolysis as a potential tool towards drug release.

Through a multi-step synthesis, two types of β-lactamase-responsive monomers were synthesized. The attachment of **6** to 7-ACA provides access for polymerization, which has yet to be reported for cephalosporin-based monomers. In summary, we have shown that 7-ACA can be synthetically modified to afford various cephalosporin-based analogs including drug conjugates.

2.3 –Disease-Associated Protease Peptide Substrate Monomer Synthesis

Towards the synthesis of enzyme-responsive monomers, various enzyme substrates were explored beyond the β-lactamase cephalosporin-based system. Therefore, alongside developing monomers that are receptive to a bacterial enzyme, we also focused our attention on the synthesis of monomers cleaved by the endogenous proteases associated with cancer. Towards the involvement of proteases in cancer development, MT1-MMP was the choice of enzyme, as certain cancer cells overexpress the protease.[7-9] Thus we set out to synthesize a peptide-substrate monomer **3**, specific for MT1-MMP.

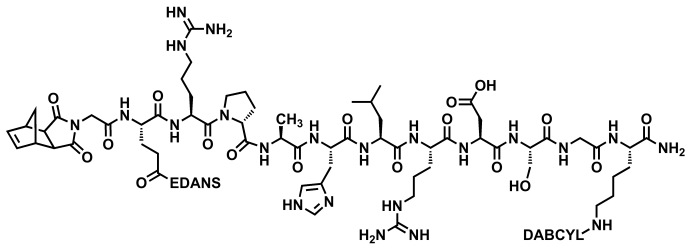

3

Figure 2.8: Structure of monomer **3**.

2.3.1 – Strategy and Design of a Dye-Labeled Peptide Monomer

In the design of diseased-associated protease peptide substrates, **CRPAHLRDSG** was the sequence selected as the basis for monomer **2**. The sequence was carefully chosen for the reported enhanced enzyme-substrate activity[3], in which the cut site is between the histidine and leucine. With respect towards the ruthenium catalyst, cysteine was purposely excluded to avoid inhibiting the metal catalyst complex. Therefore, a modified substrate was prepared with the sequence **RPAHLRDSG**. To monitor MTI-MMP hydrolysis, 5-((2-Aminoethyl)amino)naphthalene-1-sulfonic acid (EDANS) and 4,4 -Dimethylamino-azobenzene-4'-carboxylic acid (DABCYL) dyes were incorporated as fluorescence resonance energy transfer (FRET) pairs. The FRET labeled peptide substrate provides a method for detecting protease cleavage of the substrate via increased fluorescence of the donor and decreased florescence of the acceptor.[4] We note, that the catalytic domain of the membrane protease MT1-MMP is commercially available, making initial activity studies accessible in the absence of cells. To optimize the cut site accessibility, the dye-labeled amino acids were placed at each end of the enhanced peptide substrate sequence. Specifically, EDANS was attached at the amino terminus while DABCYL was attached at the carboxyl terminus. The logic behind the location of the dyes enables the visualization of the fluorescent polymer backbone upon protease cleavage. To introduce a polymerizing moiety, norbornene glycine **5** was capped at the amino terminus.

To synthesize an intricate and complex dye-labeled peptide monomer, our design was orthogonal and systematic. Either specialized dye-labeled amino acids were directly

incorporated or post-modification conjugation was carried out in attaching such dyes to the side chain residues. An amino acid side chain containing a nucleophile for conjugation was needed, in which Fmoc-Lys(ivDde)-OH was a great candidate towards this strategy. The ivDde protecting group was selectively deprotected while maintaining the integrity of various amino acid protecting groups and DABCYL was later conjugated. This method of dye conjugation was executed to preserve material and reduce the cost of synthesis. In contrast, Glu-(EDANS)-OH was directly conjugated towards nearing the end of peptide synthesis. By checking the loading before coupling the dye-labled glutamic acid, we were able to preserve the amount of material used by using a more accurate stoichiometric ratio.

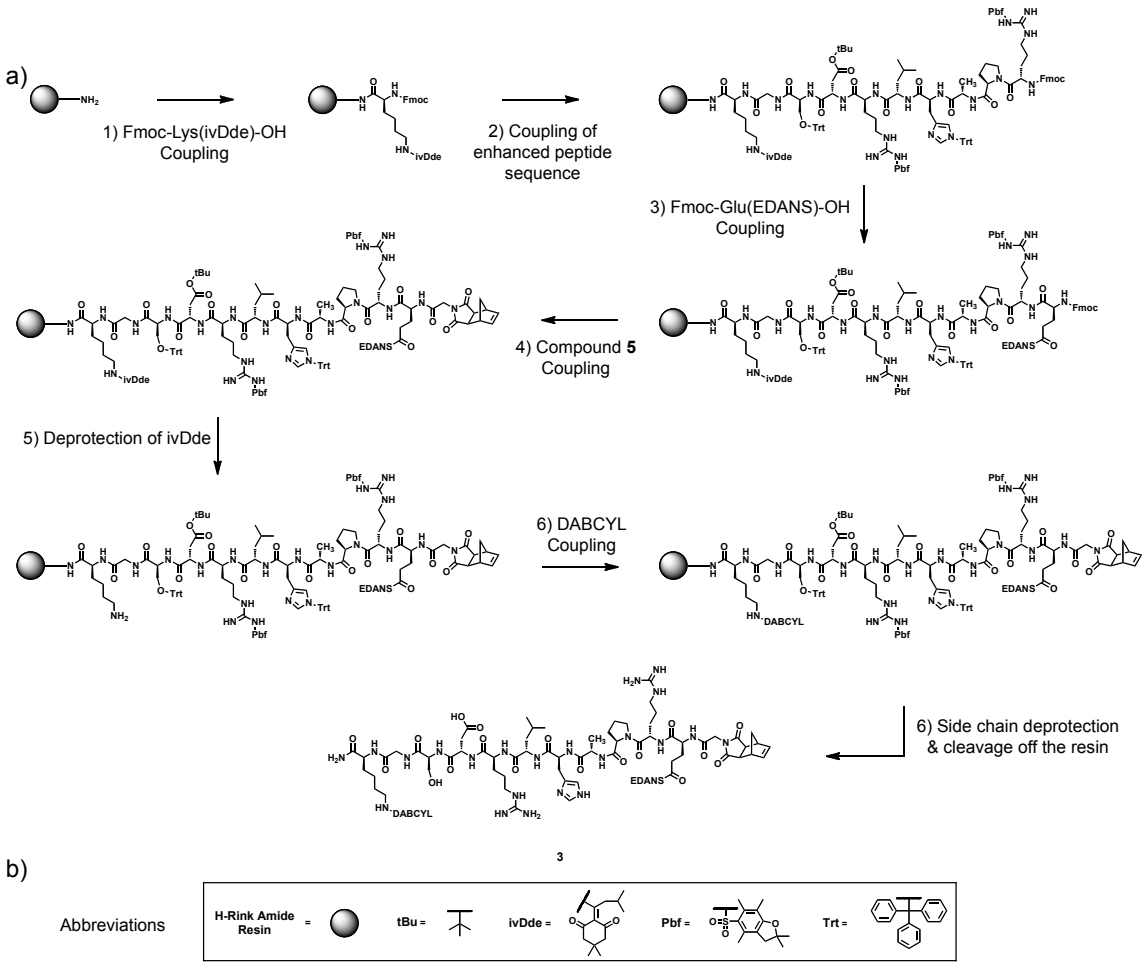

Figure 2.9: Synthesis of monomer **3**. a) Synthetic scheme of monomer **3**. b) Abbreviations of resin and protecting groups.

Monomer **3** was synthesized via standard Fmoc-based solid-phase synthesis procedures. To incorporate DABCYL, Fmoc-Lys(ivDde)-OH was first coupled to the resin and the dye was later conjugated on solid support. Starting at the C-terminus, the amino acids from the enhanced peptide sequence (**RPAHLRDSG**) were then coupled followed by Fmoc-Lys(5/6-FAM)-OH and capped by compound **5** at the terminus. The ivDde protecting group was selectively deprotected using 5% hydrazine in DMF and the

free lysine was coupled to DABCYL. Monomer **3** was cleaved from resin, purified by high performance liquid chromatography, and confirmed by mass spectrometry.

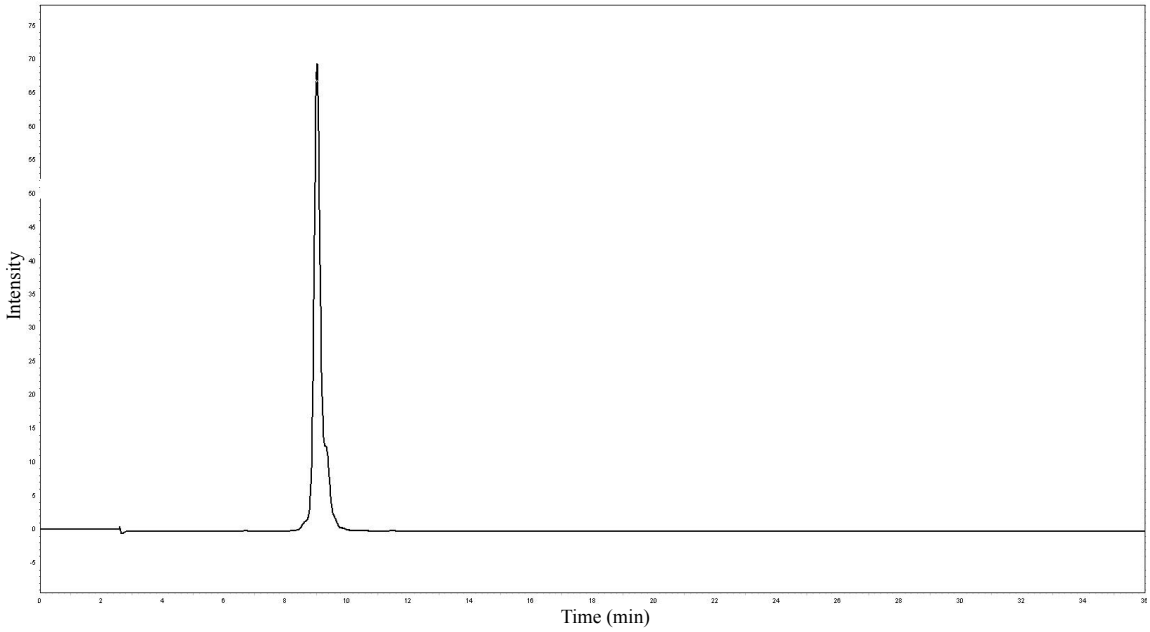

Figure 2.10: Analytical HPLC of monomer **3** following purification from the crude mixture by preparative HPLC.

As a result, the combined data shows that the disease-associated peptide substrate monomer **3** can be synthesized via solid-phase synthesis. Moreover, we show that dyes can be incorporated in the peptide sequence through either direct coupling or post-modification procedures.

2.4 –Acid Labile Doxorubicin Prodrug Monomer

In designing an acid labile doxorubicin prodrug monomer, the linker of particular interest is the carbamate functional group. Under acidic environments, the carbamate

releases carbon dioxide in conjunction with doxorubicin.[10] The pH sensitivity of carbamates provides an alternative means for the triggering of prodrug activation on top of the previously described β-lactamase-responsive and MT1-MMP peptide substrate systems. With respect towards therapy, endosomes decrease in pH as they progress towards lysosome development.[11] Utilizing the acidic conditions within the endosome of cancer cells, we aimed to develop an acid labile doxorubicin prodrug monomer for endosomal escape and drug release as an eventual control to contrast and compare with out enzymatic systems. Herein, we describe the synthesis of acid labile doxorubicin prodrug monomer **4**.

In contrast towards the synthesis of enzyme-responsive monomers, we aspired to synthesize a stimuli-responsive monomer capable of cleavage by a different mechanism control. As an alternative, ethanolamine was conjugated to norbornene anhydride to obtain compound **16**. Compound **16** provided a free hydroxyl to hydrolyze 1-ethylchloro chloroformate to afford compound **17** as shown in **Figure 2.11**. After introducing the carbonate, doxorubicin was simply attached to form the acid labile doxorubicin prodrug monomer **4**. The conjugation of doxorubicin drug with **17** was carried out using DMF as the reaction solvent due to the limited solubility of doxorubicin. The synthesis of **4** was carried out in a total of 3 steps.

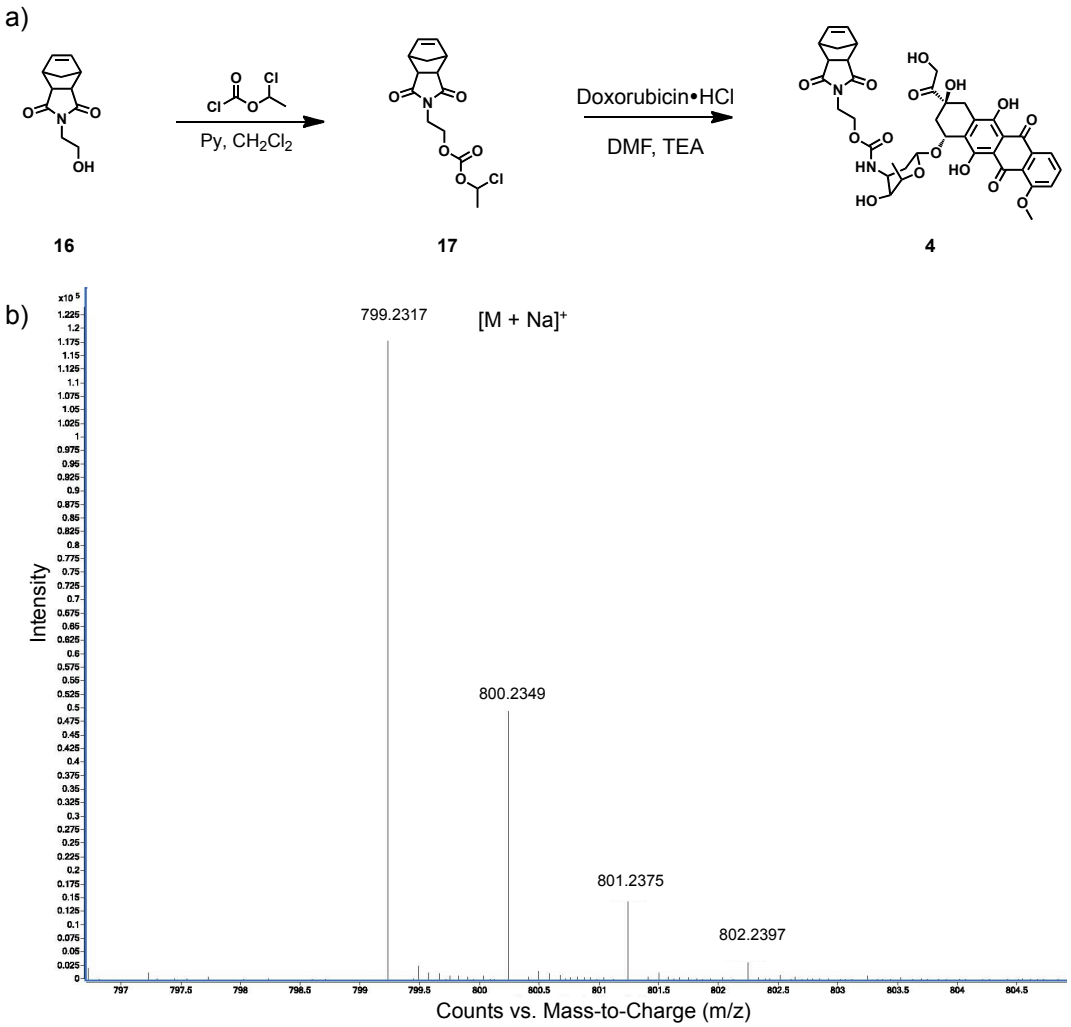

Figure 2.11: Synthesis of monomer **4**. a) Synthetic scheme of monomer **4**. b) HRMS confirmation of monomer **4**.

In the characterization of monomer **4**, the spectral assignment of ^{1}H NMR was difficult due to a forest of overlapping peaks. To confirm the conjugation of doxorubicin to with **17**, we paid close attention to the chemical shifts of both starting materials that were distinct and isolated. Specifically, the chemical shifts as well as integration of the norbornene olefins resonances, methoxy and aromatics of doxorubicin were key in the

characterization of **4**. Comparing the integration of the norbornene olefins to the aromatic protons confirm the successful conjugation of doxorubicin.

Monomer **4** was also characterized by carbon-13 nuclear magnetic resonance (^{13}C NMR), however the spectrum was also difficult to assign. To better characterize the complex monomer, other NMR experiments must be carried out such using ^{13}C distortionless enhancement by polarization transfer (DEPT) spectral analysis. Using these techniques, the separation of primary, secondary, tertiary, and quaternary carbons would be advantageous in assigning the carbon spectra. Due to the difficulties of both ^{1}H NMR and ^{13}C NMR spectra, monomer **4** was further confirmed by HRMS. Despite the inability to fully assign NMR spectra, through the preliminary NMR data in combination with mass spectrometry we were able to confirm the synthesis of acid labile prodrug monomer **4**.

2.5 – Conclusions

In this chapter, we have described the synthesis of stimuli-responsive monomers **1-4.** Here we showed that β-lactamase-responsive monomers that contain a hydrophilic moiety as well as doxorubicin prodrug could be synthesized. Furthermore, we have shown that dyes can be integrated within the synthesis of peptide substrates for the detection of diseased tissues and cancer cells. Lastly, we have also shown the synthesis of acid labile doxorubicin prodrug monomer for the hypothetical endosomal escape via low pH. The synthesis of monomers **1-4** provide the basic building blocks of monomers towards the synthesis and design of highly functionalized polymers for the goal of

enzyme-directed assembly of nanomaterials, disease detection, and prodrug delivery as described in Chapter 3.

2.6 – Experimental

2.6.1 – General Methods/Instrument Details

All reagents were purchased from Sigma-Aldrich, TCI America, and other commercial sources and used without further purification unless otherwise noted. Dry DCM solvent was obtained using a Dow-Grubbs two-column purification system (Classcontour System, Irvine, CA). Dry DMF and THF were distilled from calcium hydride. Deuterated solvents were purchased from Cambridge Isotopes Laboratories Inc. All other solvents were used as is without further purification. Reactions were monitored by thin-layer chromatography (TLC) performed on pre-coated silica gel plates. All air-sensitive experiments to were carried out using Schlenk flask procedures under nitrogen atmosphere. Chromatography purification of products was accomplished using flash chromatography on silica gel 60 (230-400 mesh). Analytical HPLC analysis and semi-prep purification were performed on Jupiter 4u Proteo 90A Phenomenex columns (150 x 4.60 mm & 250 x 10.00 mm, respectively) with a binary gradient using a Hitachi-Elite LaChrom L-2130 pump equipped with UV-Vis detector (Hitachi-Elite LaChrom L-2420). Prep-HPLC purification on monomer **4** was performed on a Waters Delta Prep 300 using a Jupiter 4u Proteo 90A Phenomenex column (250 x 21.20 mm). Products were lyophilized using a Labconoco Freezone 2.5 Plus lyophilizer. To confirm molecular weights, mass spectra was performed on an Agilent 6230 HR-ESI-TOF MS provided by the Mass Spectrometry Facility at UCSD Department of Chemistry & Biochemistry.All

NMR spectra were recorded on Varian Mercury 300Mhz, 400Mhz, and Joel 500Mhz spectrometers. All NMR spectra were recorded in $CDCl_3$, CD_2Cl_2, DMSO-d_7, and chemical shifts are reported in δ (ppm) relative to the respective deuterated solvent.

2.6.2 – Synthesis

(6*R*,7*R*)-*tert*-butyl 7-(2-(1,3-dioxo-3a,4,7,7a-tetrahydro-1*H*-4,7-methanoisoindol-2(3*H*)-yl)acetamido)-8-oxo-3-(3-oxo-2,7,10,13,16-pentaoxa-4-azaheptadecyl)-5-thia-1-azabicyclo[4.2.0]oct-2-ene-2-carboxylate (1). Compound **10** (1.18g, 1.98mmol) was dissolved in dichloromethane (100mL) and PEG-amine (400µL, 1.93mmol) was added. N-N-Diisopropyletheylamine (500µL, 2.87mmol) was added drop wise and reaction was stirred over night for 24 hours. The reaction mixture was washed with 0.5N HCl (50mL) and deionized water (2x50mL). The organic layers were combined, dried over Na_2SO_4, gravity filtered, and concentrated *in vacuo* to afford yellow foam solid. The material was further purified via flash column chromatography eluting unreacted Compound **10** using 4:1 EtOAc/CH_2Cl_2 and flushing the column with 8:1.5:0.5 EtOAc/CH_2Cl_2/MeOH to collect impure product. The material was further purified by HPLC using semi-prep column and lyophilized to give compound **1** as a white solid (481.2mg 0.66mmol, 33.65%). **Figure 2.12**: Gradient: 35-40% B from 3-34 minutes, 40-90% B from 34-40 minutes, 90% B from 40-45 minutes, 90-35% B from 45-50 minutes, wavelength: 214nm, flow rate: 1 mL/min). R_f 0.35 (8:1.5:0.5 EtOAc/CH_2Cl_2/MeOH); **Figure 2.13**: ^{1}H NMR (400MHz, CD_2Cl_2): δ 1.47 (s, 3H), 1.51 (s, 9H), 1.68 (d, 1H), 2.03 (s, 2H), 2.12 (s, 2H) 2.75 (s 2H), 3.26 (s 2H), 3.34-3.55 (m, 12H), 3.59 (s, 9H), 4.16 (d, 4H), 4.22 (d, 1H), 4.79 (d, 1H), 4.99 (d, 1H), 5.02 (d, 1H), 5.28 (d, 1H), 5.48 (bs, 1H), 5.57 (bs, 1H), 5.77

(dd, 1H), 6.30 (s, 2H), 6.42 (s, 2H), 6.42 (d, 1H), 6.81 (dd, 1H); ^{13}C NMR (500MHz, $CDCl_3$): δ 26.13, 27.83, 40.72, 42.95, 45.35, 48.09, 57.33, 58.99, 69.91, 70.46, 71.83, 83.83, 125.03, 126.77, 138.07, 156.02, 160.38, 163.95, 166.39, 177.52; HRMS (M+Na): calculated: 745.2725; found 745.2730.

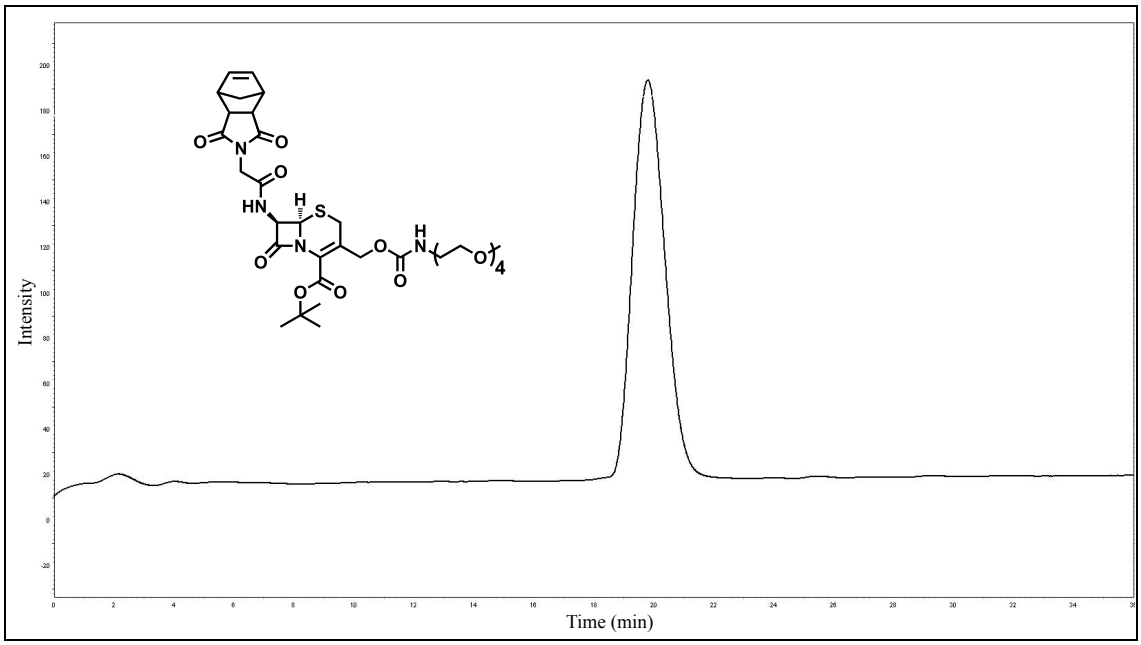

Figure 2.12: HPLC trace of monomer **1**.

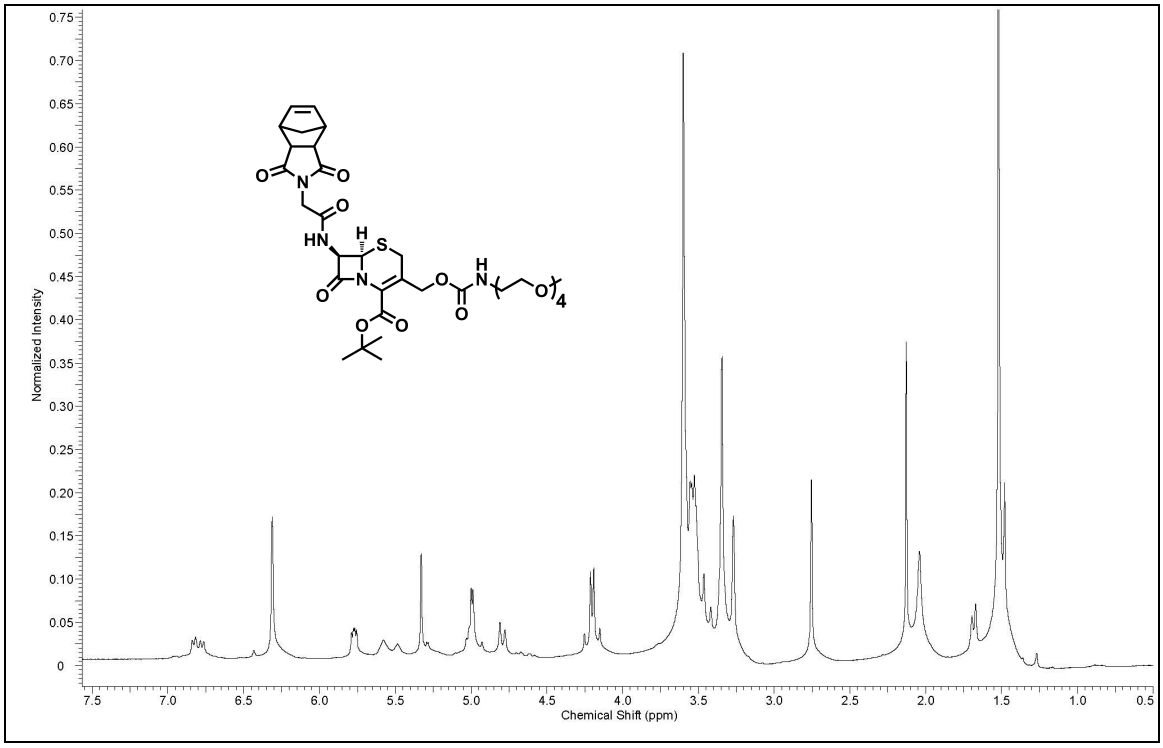

Figure 2.13: ^{1}H NMR of **1**.

(6*R*,7*R*)-*tert*-butyl 7-(2-(1,3-dioxo-3a,4,7,7a-tetrahydro-1*H*-4,7-methanoisoindol-2(3*H*)-yl)acetamido)-3-(((((2*S*,3*S*,4*S*,6*R*)-3-hydroxy-2-methyl-6-(((1*R*,3*R*)-3,5,12-trihydroxy-3-(2-hydroxyacetyl)-10-methoxy-6,11-dioxo-1,2,3,4,6,11-hexahydrotetracen-1-yl)oxy)tetrahydro-2*H*-pyran-4-yl)carbamoyl)oxy)methyl)-8-oxo-5-thia-1-azabicyclo[4.2.0]oct-2-ene-2-carboxylate (2). To a foil wrapped Schlenk flask, compound **10** (25.20mg, 0.042mmol) and doxorubicin•HCl (20.06mg, 0.035mmol) were dissolved in DMF (1.7μL). TEA was added drop wise and the reaction was stirred for 18 hours under nitrogen gas. DMF solvent was removed under reduced pressure and re-dissolved in DCM. The organic layer was washed with deionized water (3 x 20ml) and concentrated *in vacuo*. The material was partially purified via flash chromatography

using 8.5:1.0:0.5 EtOAc/CH_2Cl_2/MeOH to recover unreacted **10**. The remaining product was collected, concentrated, and purified by HPLC to yield a red powder (34.03mg, 0.032mmol, 76.01%). **Figure 2.14**: Gradient: 30-67% B from 3-33 minutes, 67-90% B from 33-38 minutes, 90% B from 40-42 minutes, 90-0% B from 45-50 minutes, wavelength: 214nm, flow rate: 1 mL/min). R_f 0.18 (8:1.5:0.5 EtOAc/CH_2Cl_2/MeOH; **Figure 2.15**: ^{1}H NMR (500MHz, $CDCl_3$): δ 1.51 (s, 12H), 2.63 (s, 1H), 2.78 (s, 2H), 3.04-3.18 (m, 4H), 3.29 (s, 1H), 3.33 (d, 2H), 3.48 (d, 2H), 3.50 (d, 2H), 3.66 (s, 1H), 3.82 (d 2H), 4.10 (s, 3H), 4.15 (d, 1H), 4.19 (s, 1H), 4.25 (s, 2H), 4.43 (d, 1H), 4.69 (d, 1H), 4.78 (s, 2H), 5.17 (d, 1H), 5.98 (dd, 1H), 6.30 (2H), 6.92 (d, 1H), 7.06 (s, 1H), 7.19 (d, 1H), 7.43 (d, 1H), 7.43 (d, 1H), 7.48 (s, 1H), 7.82 (t, 1H), 8.03 (s, 1H), 8.07 (d, 1H); ESI-*m/z* 1081.4 $[M+Na]^+$.

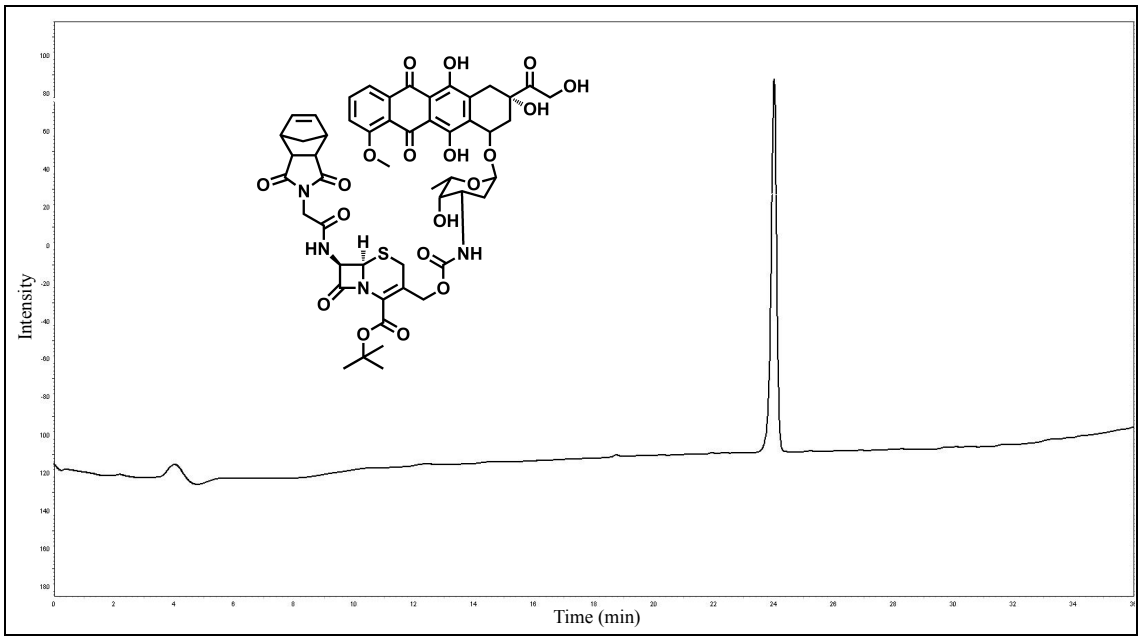

Figure 2.14: HPLC trace of monomer **2**.

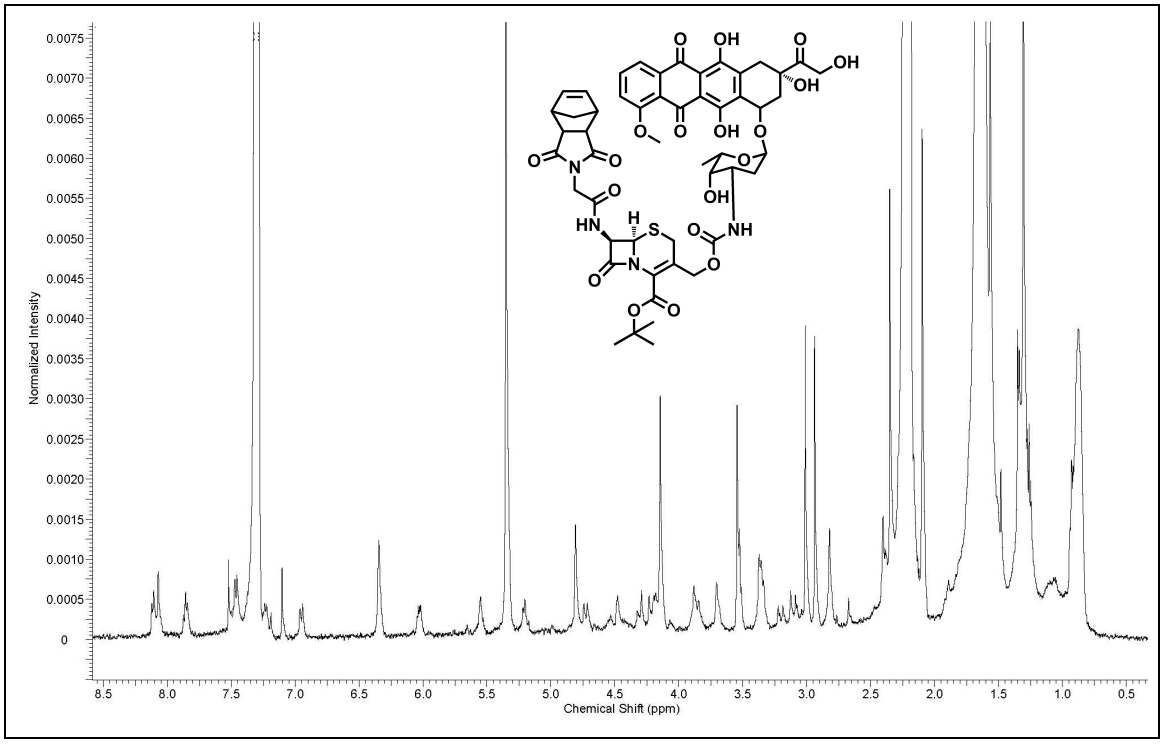

Figure 2.15: ^{1}H NMR of **2**.

N-(Glu(EDANS)-Arg-Pro-His-Leu-Arg-Asp-Ser-Gly-Lys(DABCYL)-*cis*-5-norbornene-*exo*-dicarboimide (3). Monomer **3** was synthesized standard Fmoc-based solid phase peptide synthesis procedures using Rink Amide resin. Fmoc deprotection was performed with 20% piperidine in DMF (1 x 3 min) and (1 x 10 min). Coupling of Fmoc-Lys(ivDde)-OH was carried out with HATU and DIPEA (resin/amino acid/ HATU/DIPEA 1:5:4.9:10). Consecutive MT1-MMP enhanced amino acid sequence was coupled in the same fashion using HBTU as the coupling reagent. (1:4:3.9:8). Fmoc-Glu(EDANS)-OH (1:4:3.9:8) and norbornene-glycine **5** (1:4:3.9:8) were coupled respectively. ivDde protected lysine was deprotected with 5% hydrazine in DMF and a 5 mg sample was analyzed for free amines by the ninhydrin test. Sample was analyzed by

UV nanodrop at wavelength 214 nm. DABCYL was coupled to the free lysine using HBTU and DIPEA (1:4:3.9:8). **2** was cleaved from the resin by trifluoroacetic acid/water/TIS (95:2.5:2.5) for 2 hours. The resin was washed with TFA, the combined organics were concentrated, and precipitated in cold ether to afford an red solid. The cleaved peptide was then purified by HPLC. **Figure 2.10**: Gradient: 30-45% B from 3-33 minutes, 34-85% B from 34-38 minutes, 85% B from 38-40 minutes, 85-0% B from 40-48 minutes, wavelength: 472nm, flow rate: 1 mL/min). ESI-*m/z* 984.44 $[M+2H]^{2+}$.

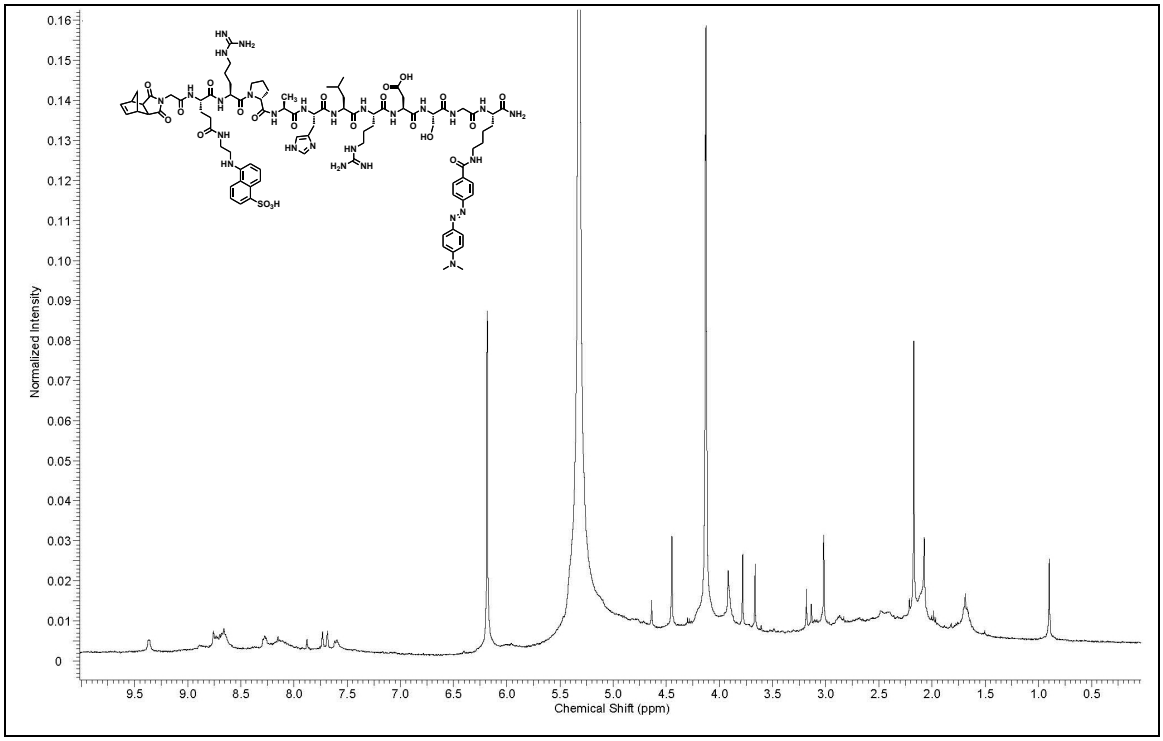

Figure 2.16: ^{1}H NMR of monomer **3**.

2-(1,3-dioxo-3a,4,7,7a-tetrahydro-1H-4,7-methanoisoindol-2(3H)-yl)ethyl ((2R,3R,4S,6R)-3-hydroxy-2-methyl-6-(((1R,3R)-3,5,12-trihydroxy-3-(2-hydroxyacetyl)-10-methoxy-6,11-dioxo-1,2,3,4,6,11-hexahydrotetracen-1-

yl)oxy)tetrahydro-2H-pyran-4-yl)Carbamate (4). To a Shlenk flask under nitrogen gas covered in foil, compound **17** (245.0mg, 0.78mmol) and doxorubicin-HCl (257.9mg, 0.44mmol) were dissolved in dry DMF (15mL). TEA (125µL, 0.89mmol) was added drop wise and the reaction was stirred over night for 22 hours. The solvent was removed under reduced pressure, re-dissolved with DCM, and washed with deionized water (3 x 100ml). The organic layer was concentrated *in vacuo*, and purified via flash chromatography using 8.5:1.0:0.5 EtOAc/CH_2Cl_2/MeOH. Material was further purified by HPLC using gradient 30-45% buffer B over 30 mins. The product was collected and lyophilized to afford a red powder (409.6mg, 0.53mmol 67.53%). **Figure 2.17**: Gradient: 15-67% B from 3-33 minutes, 67-85% B from 34-38 minutes, 85% B from 38-40 minutes, 85-0% B from 40-48 minutes, wavelength: 600nm, flow rate: 1 mL/min). R_f 0.5 (8.5:1.0:0.5 EtOAc/CH_2Cl_2/MeOH); **Figure 2.18**:^{1}H NMR (400MHz, $CDCl_3$): δ 1.29 (d, 2H), 1.35 (d, 3H), 1.53 (d, 1H), 1.74-1.87 (m, 3H), 2.16 (d, 1H), 2.19 (d, 1H), 2.37 (d, 2H), 2.55 (m, 5H), 2.71 (s, 2H), 3.03 (d, 2H), 3.26 (s, 2H), 3.29 (d, 2H), 3.58-3.61 (m, 1H), 4.10 (d, 1H), 4.08 (s, 3H), 4.12 (d, 1H), 4.38-4.41 (m, 1H), 4.74 (d, 1H), 4.78 (s, 2H), 5.31 (s, 1H), 5.54 (s, 1H), 6.29 (s, 2H), 7.40 (d, 1H), 7.79 (t, 1H), 8.04 (d, 1H); **Figure 2.19**: ^{13}C NMR (400MHz, $CDCl_3$): δ 16.68, 29.13, 33.64, 35.27, 37.60, 42.36, 44.87, 47.53, 56.35, 61.33, 65.24, 66.76, 67.73, 69.22, 100.36, 111.05, 118.08, 119.52, 120.53, 133.33, 135.47, 137.46, 155.37, 160.71, 177.91, 178.33, 186.37, 186.80, 213.58; HRMS (M + Na): calculated: 799.2321; found 799.2317.

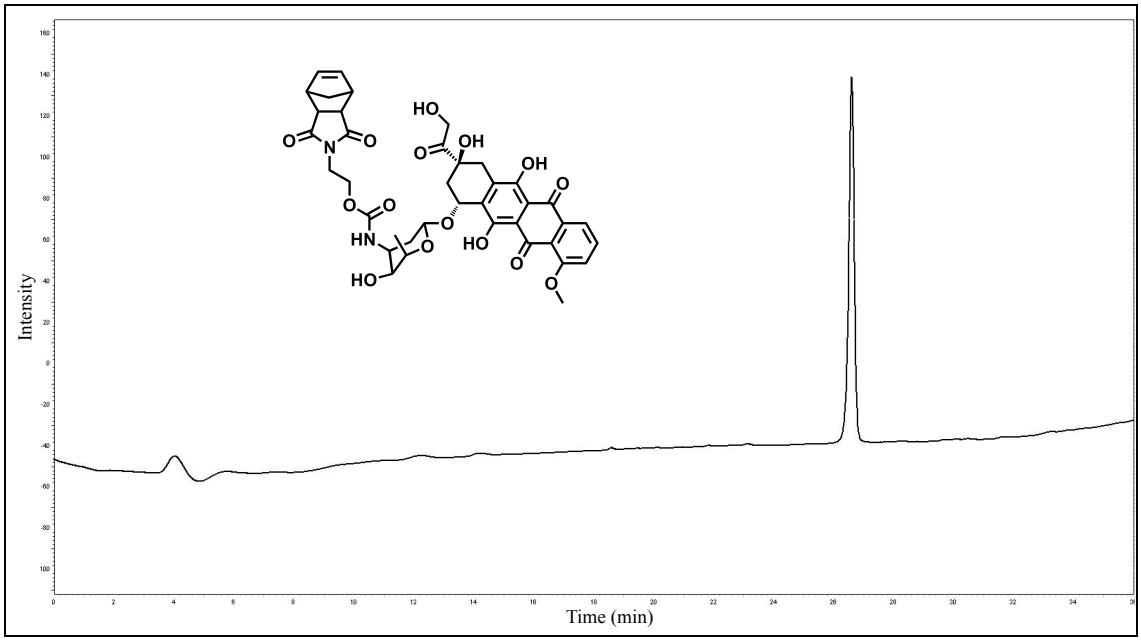

Figure 2.17: HPLC trace of monomer **4**.

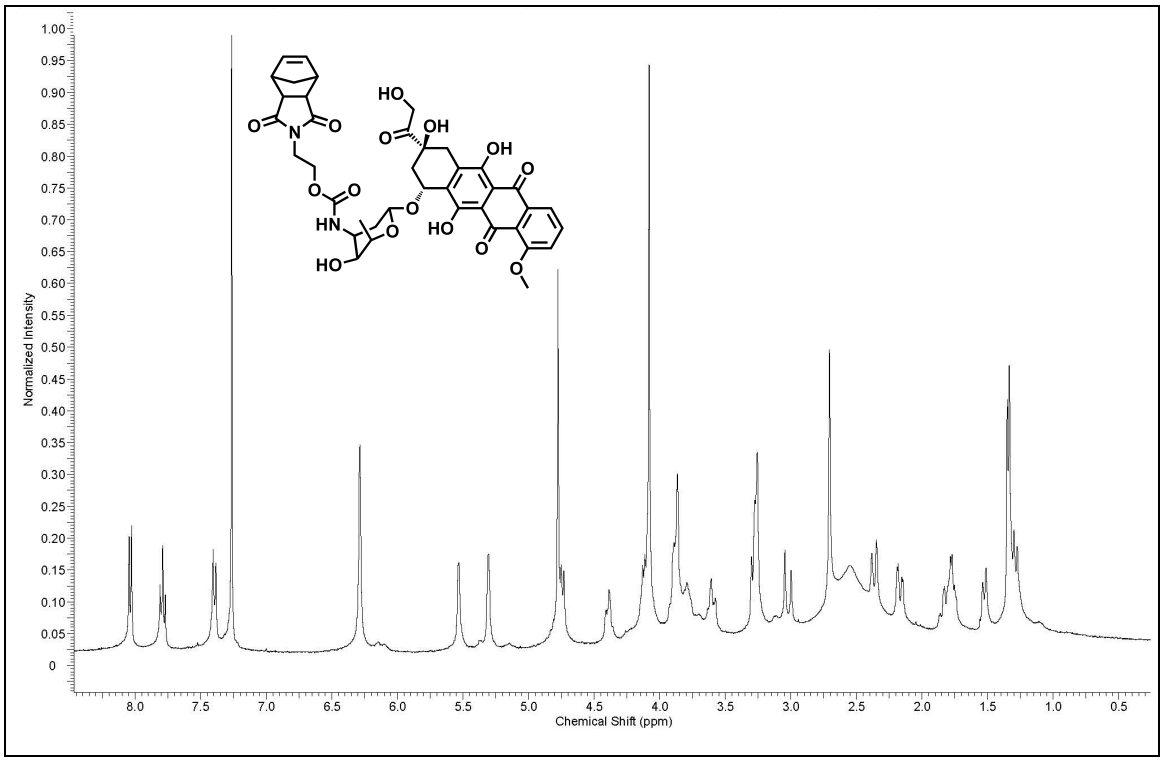

Figure 2.18: ^{1}H NMR of **4**.

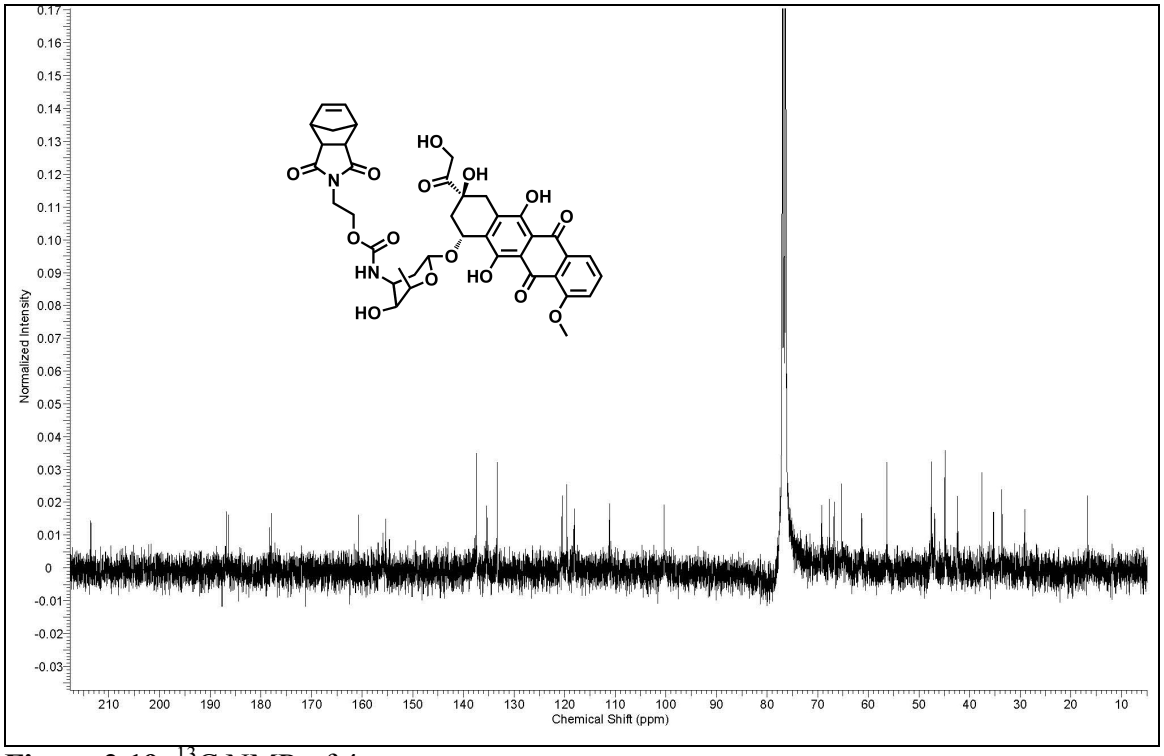

Figure 2.19: ^{13}C NMR of **4**.

N-(Glycine)-*cis*-5-norbornene-*exo*-dicarboximide (5). To a round bottom flask, *cis*-5-*exo*-2,3-dicarboxylic anhydride (5.000g, 30.48mmol) and glycine (3.03953g, 40.50mmol) were suspended in toluene (30 mL). Using a Dean Stark strap, the reaction was refluxed for 12 hours. The reaction mixture was removed from the oil bath, cooled to room temperature and the solvent was removed *in vacuo*. The remaining residue was dissolved with EtOAc (60 mL), washed with 0.2 N aqueous HCl (2 x 20mL), and concentrated under reduced pressure. The residue was dissolved in saturated $NaHCO_3$ solution, washed with CH_2Cl_2 (2 x 20mL), and acidified to pH 2 using roughly 4 mL of concentrated HCl. Upon acidification, a white precipitate was observed. The aqueous layer was extracted with $CHCl_3$ (3 x 50mL), the organic layer were collected, dried over Na_2SO_4, gravity filtered, and concentrated *in vacuo* to afford a white powder (5.36g,

24.23mmol, 79.50%); **Figure 2.20**: ^{1}H NMR (400MHz, $CDCl_3$): δ 1.53 (d, 1H), 1.64 (d, 1H), 2.78 (s, 2H), 3.33 (d, 2H), 4.30 (d, 2H), 6.32 (d, 2H)

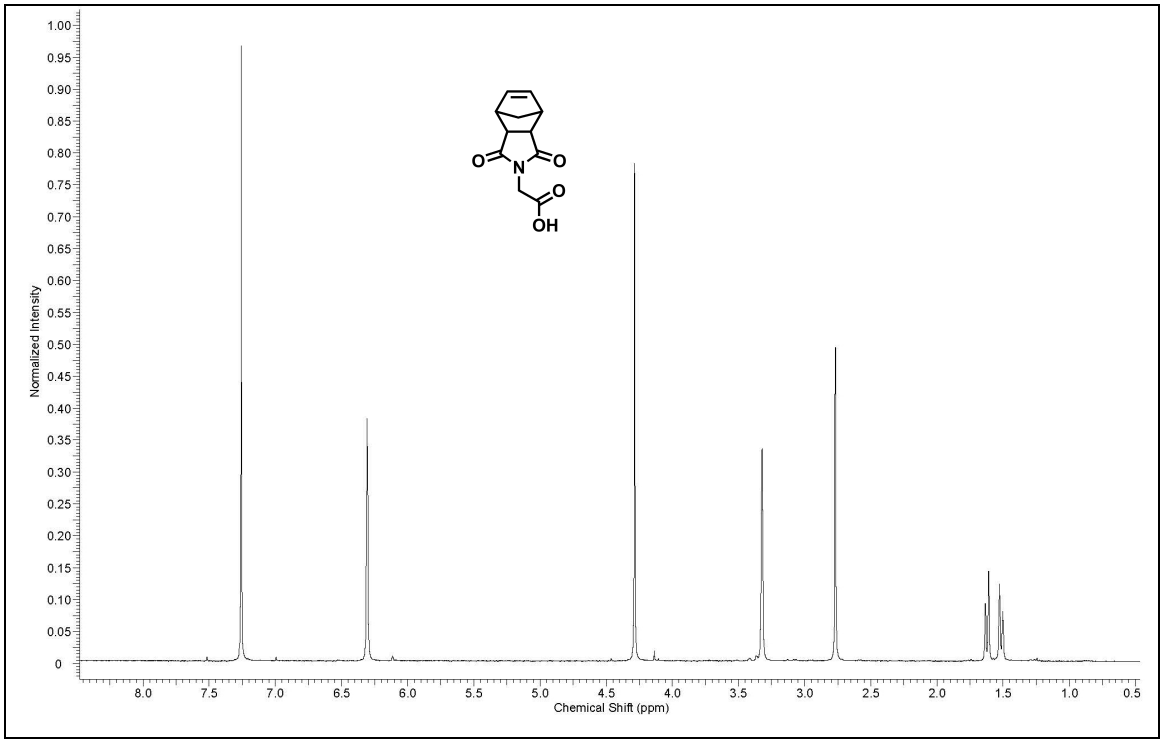

Figure 2.20: ^{1}H NMR of **5**.

2-(1,3-dioxo-3a,4,7,7a-tetrahydro-1H-4,7-methanoisoindol-2(3H)-yl)acetyl chloride (6). To a Schlenk flask under nitrogen gas containing norbornene glycine (4.08g, 18.44mmol), dry dichloromethane (66mL) was added via needle and syringe. The dissolved solution was then refluxed over an oil bath after the drop wise addition of thionyl chloride (2.5mL, 34.42mmol). After 4 hours of refluxing, the solvent was removed *in vacuo* to afford a white solid (4.35g, 18.15mmol, 98.43%). **Figure 2.21**: ^{1}H NMR (400MHz, $CDCl_3$): δ 1.57 (s, 2H), 2.80 (s, 2H), 3.35 (s, 2H), 4.63 (s, 2H), 6.33 (s, 2H); ESI-*m/z* 351.5 $[M+Na]^{+}$.

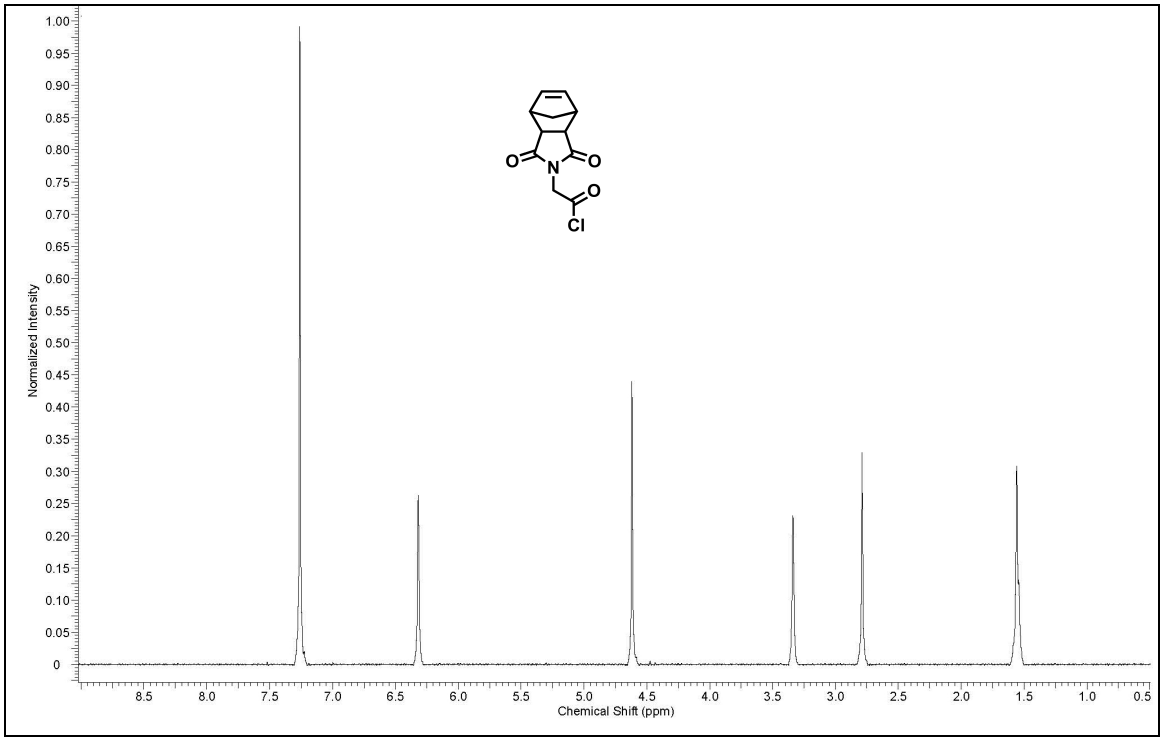

Figure 2.21: ^{1}H NMR of **6**.

(6R,7R)-*tert*-Butyl 3-(acetoxymethyl)-1-amino-8-oxo-5-thia-1-azabicyclo[4.2.0]oct-2-ene-2-carboxylate (7). To a 1L round bottom flask, 7-Aminocephalosporonic acid (5.01264g, 18.410mmol) was suspended in t-butyl acetate (300mL) and *p*-Toluene sulfonic acid (3.9885g, 20.968mmol) was added. The flask was sealed with a septum and the suspension was stirred for 15 minutes. Sulfuric acid was added drop wise over 15 minutes and the reaction was allowed to stir for 7 hours. The reaction mixture was quenched with saturated $NaHCO_3$ solution until slightly basic and the organic layer was removed. The aqueous layer was extracted with EtOAC (2x50mL) and the organic layers were combined. The organic layer was dried over Na_2SO_4, filtered by gravity, and concentrated *in vacuo*. The material was purified by flash chromatography using 4:1

EtOAc/DCM to afford a yellow solid (4.08g, 12.4mmol, 67.54%). For characterization see cited paper. **Figure 2.22**: ^{1}H NMR (400MHz, $CDCl_3$): δ 1.54 (s, 9H), 1.75 (s, 2H), 2.09 (s, 3H), 3.35 (d, 1H), 3.55 (d, 1H), 4.76 (d, 1H), 4.79 (d, 1H), 4.94 (d, 1H), 5.03 (d, 1H); ESI-*m/z* 350.92 $[M+Na]^{+}$.

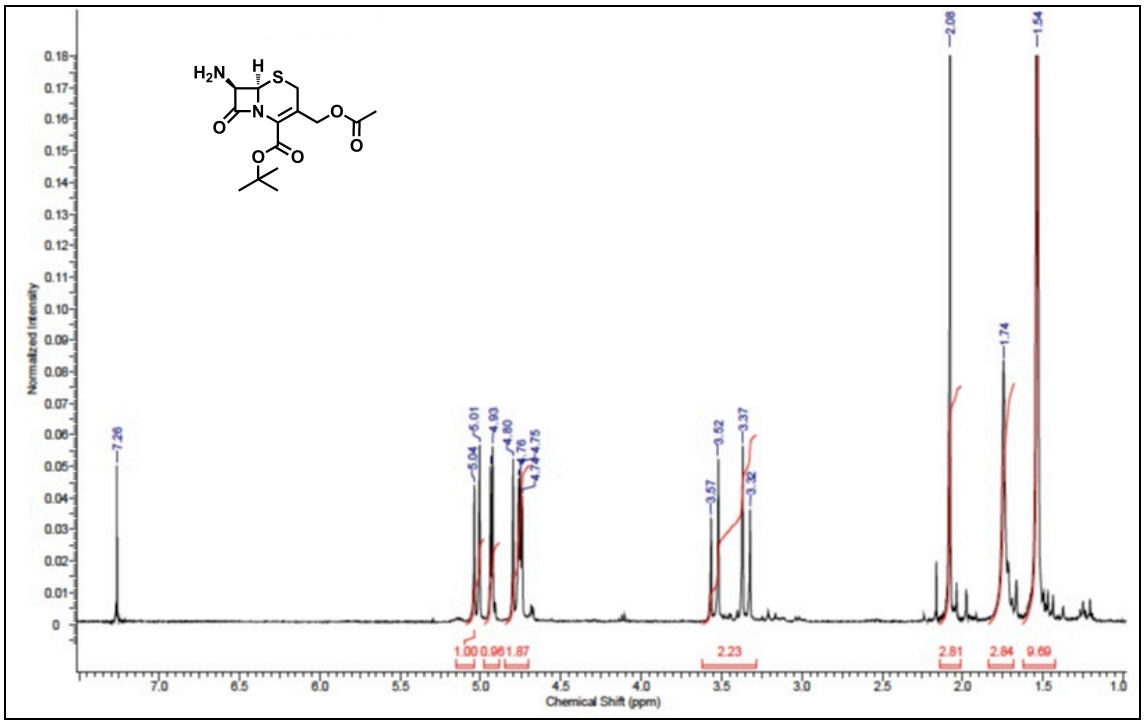

Figure 2.22: ^{1}H NMR of **7**.

(6*R*,7*R*)-*tert*-butyl 3-(acetoxymethyl)-7-(2-(1,3-dioxo-3a,4,7,7a-tetrahydro-1*H*-4,7-methanoisoindol-2(3*H*)-yl)acetamido)-8-oxo-5-thia-1-azabicyclo[4.2.0]oct-2-ene-2-carboxylate (8). Compound **3** (4.03 g, 12.3 mmol), was dissolved in DCM (80) and saturated $NaHCO_3$ solution (20mL) was added. The solvent mixture was stirred over an ice bath for 15 minutes. Separately, norbornene acyl chloride, (4.35g, 18.2mmol), was dissolved in dry dichloromethane and added drop wise to reaction mixture under nitrogen

gas via cannula. The reaction was stirred vigorously for 4 hours upon which the aqueous portion was removed. The organic layer was washed with saturated $NaHCO_3$ solution (2 X 30mL), brine (30mL), dried over $MgSO_4$, filtered by gravity, and the solvent was concentrated down *in vacuo*. The product was purified via flash chromatography using 3:1 EtOAc/CH_2Cl_2. Compound **2** was isolated as a yellow solid (2.83g, 5.32mmol, 43.43%). R_f 0.8 (3:1 EtOAc/CH_2Cl_2); **Figure 2.23**: ^{1}H NMR (400MHz, $CDCl_3$): δ 1.52 (s, 9H), 1.65 (d, 2H), 1.70 (d, 1H), 2.09 (s, 3H), 2.76 (s, 2H), 3.31 (s, 2H), 3.37 (d, 1H), 3.54 (d, 1H), 4.24 (dd, 2H), 4.27 (s, 2H) 4.80 (d, 1H), 4.95 (d, 1H), 5.08 (d, 1H), 5.77 (dd, 1H), 6.30 (s, 2H), 7.01 (d, 1H); **Figure 2.24**: ^{13}C NMR (500MHz, $CDCl_3$): δ 20.51, 26.17, 27.50, 40.49, 42.68, 45.11, 47.74, 56.96, 58.96, 62.79, 83.73, 123.59, 137.69, 160.07, 163.69, 166.15, 170.41, 177.22; ESI-*m/z* 554.1 $[M+Na]^+$.

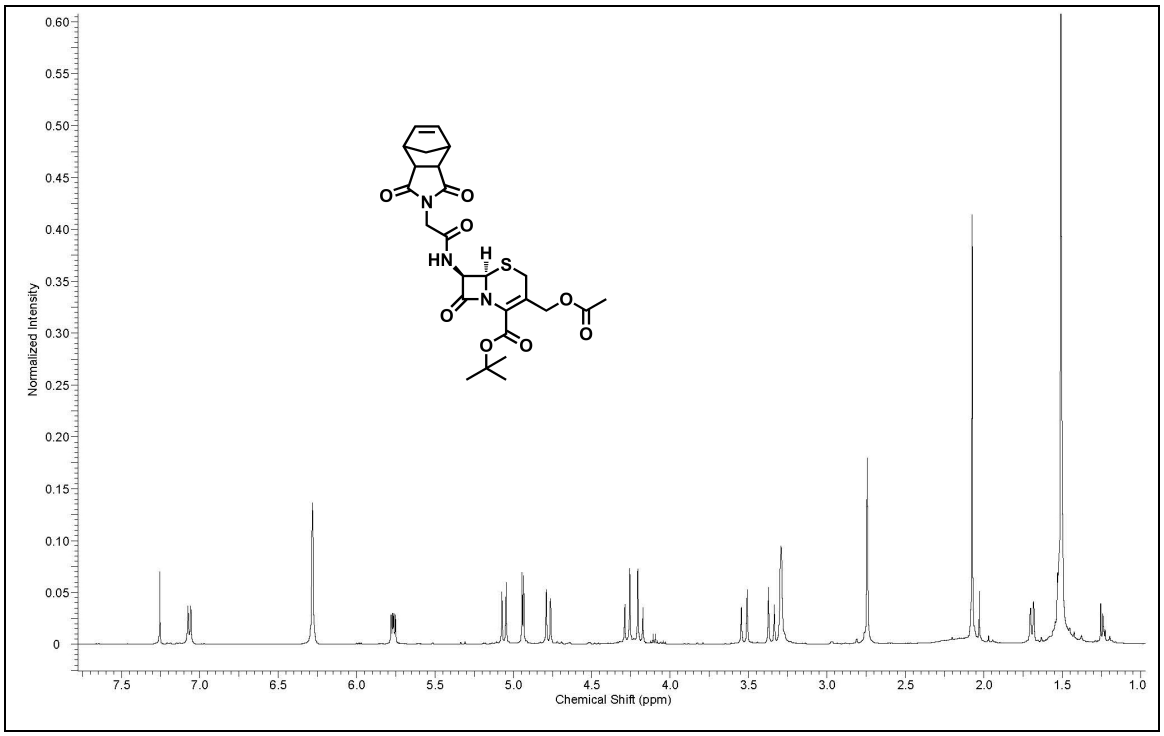

Figure 2.23: ^{1}H NMR of **8**.

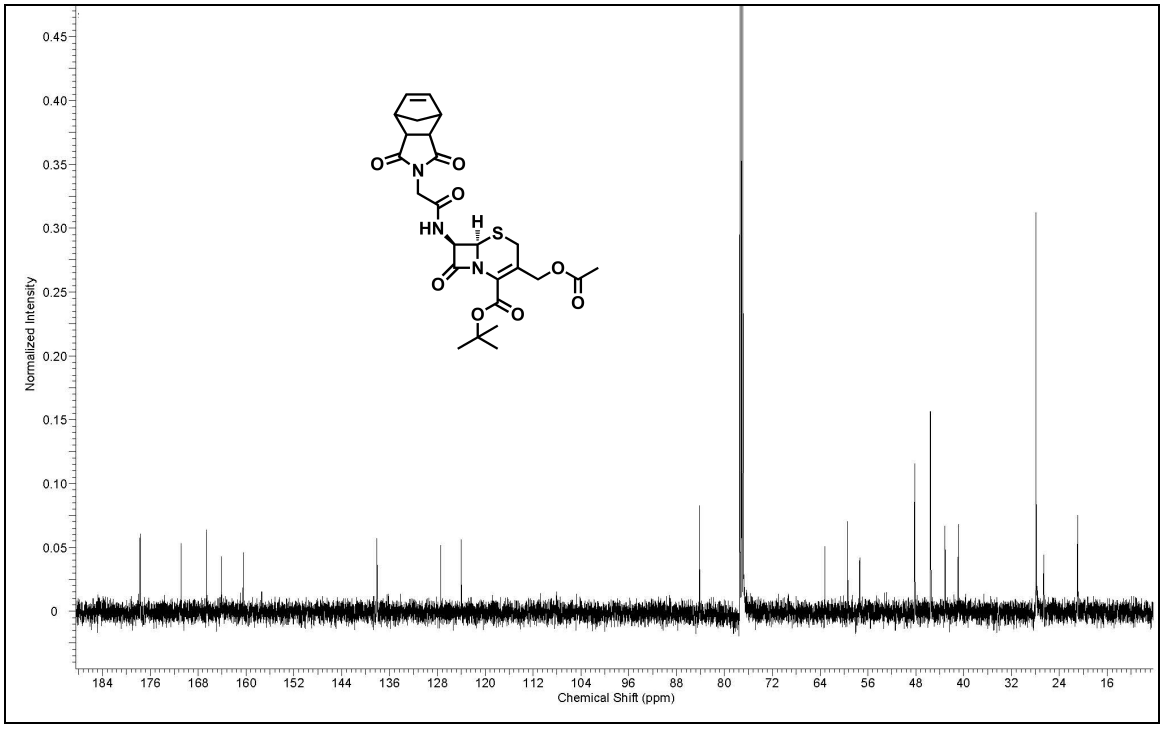

Figure 2.24: ^{13}C NMR of **8**.

(6*R*,7*R*)-*tert*-butyl 7-(2-(1,3-dioxo-3a,4,7,7a-tetrahydro-1*H*-4,7-methanoisoindol-2(3*H*)-yl)acetamido)-3-(hydroxymethyl)-8-oxo-5-thia-1-azabicyclo[4.2.0]oct-2-ene-2-carboxylate (9). To a 1L Erlenmeyer Flask containing compound **4** (2.8290g, 5.3219mmol), dry THF (31.2mL) was added to dissolve solid. Hexanes (280mL) was then added to afford a suspension in a mixture of (9:1 THF/Hexanes). CALB (1.4178g), 4Å molecular sieves (5.71g), and sec-butanol (10.3mL, 112.28mmol) were added to the suspension mixture and sealed with a septum. The reaction was shaken and incubated at 50^{o}C for 6-8 days upon which solid stuck to the sides of the flask was scraped daily. Upon completion, the reaction was dissolved in dichloromethane and filtered by vacuum filtration to remove molecular sieves and lipase. The solvent was removed *in vacuo* and recrystallized using chloroform/cyclohexane mixture to afford a white solid (2.1500g

4.3919mmol, 82.53%). R_f 0.5 (3:1 EtOAc/Hexanes); **Figure 2.25**: ^{1}H NMR (400MHz, $CDCl_3$): δ 1.52 (s, 9H), 1.53 (d, 1H), 1.73 (d, 1H), 2.75 (s, 2H), 3.31 (s, 2H), 3.54 (d, 1H), 3.63 (d, 1H), 3.93 (d, 1H), 4.21 (d, 1H), 4.29 (d, 1H) 4.48 (d, 1H), 4.92 (d, 1H), 5.79 (dd, 1H), 6.29 (s, 2H), 7.30 (d, 1H); ESI-*m/z* 512.3 $[M+H]^+$.

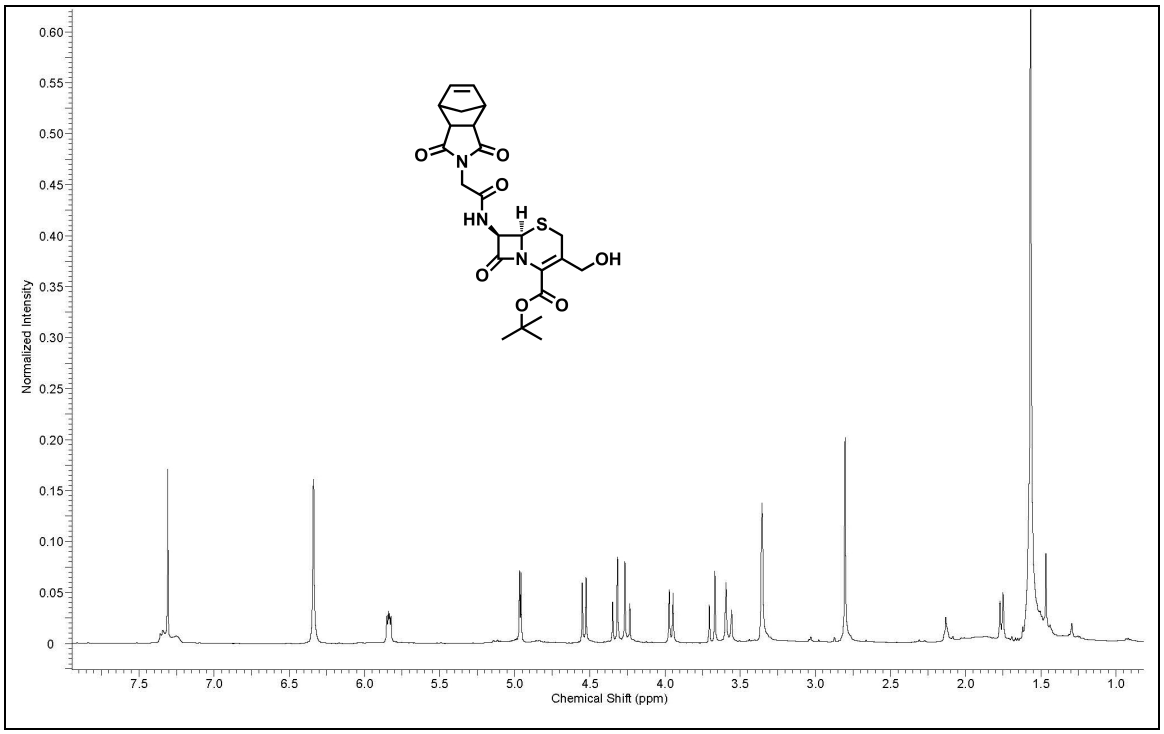

Figure 2.25: ^{1}H NMR of **9**.

(6R,7R)-tert-butyl 3-((((1-chloroethoxy)carbonyl)oxy)methyl)-7-(2-(1,3-dioxo-3a,4,7,7a-tetrahydro-1H-4,7-methanoisoindol-2(3H)-yl)acetamido)-8-oxo-5-thia-1-azabicyclo[4.2.0]oct-2-ene-2-carboxylate (10). To a Schlenk flask, compound **5** (2.0133g, 4.1127mmol) and 1-ethylchloro chloroformate (580μL, 5.3753mmol) were dissolved in dry dicholoromethane (194mL) under nitrogen using Schlenk line techniques.

Dry pyridine (450µL, 5.5860mmol) was added drop wise and reaction was stirred for 3 hours. Reaction mixture was then washed with cold 0.5N HCl (10mL) and deionized water (2 x 10mL). The organic layer was collected, dried over Na_2SO_4, filtered by gravity, and concentrated *in vacuo*. The material was purified via flash chromatography using 1:1 EtOAc/CH_2Cl_2 to afford a salmon colored solid (1.6061g, 2.6946mmol, 65.19%). R_f 0.6 (1:1 EtOAc/CH_2Cl_2); **Figure 2.26**: ^{1}H NMR (400MHz, $CDCl_3$): δ 1.54 (s, 9H), 1.62 (s, 1H), 1.70 (d, 2H), 1.84 (d, 3H), 2.77 (s, 2H), 3.33 (s, 2H), 3.59 (d, 1H), 4.19 (d, 1H), 4.29 (d, 1H), 4.93 (d, 1H), 4.97 (d, 1H), 5.23 (d, 1H), 5.29 (d, 1H), 5.82 (dd, 1H), 6.31 (s, 2H), 6.43 (q, 1H), 6.68 (d, 1H); ESI-*m/z* 620.1 $[M+Na]^+$.

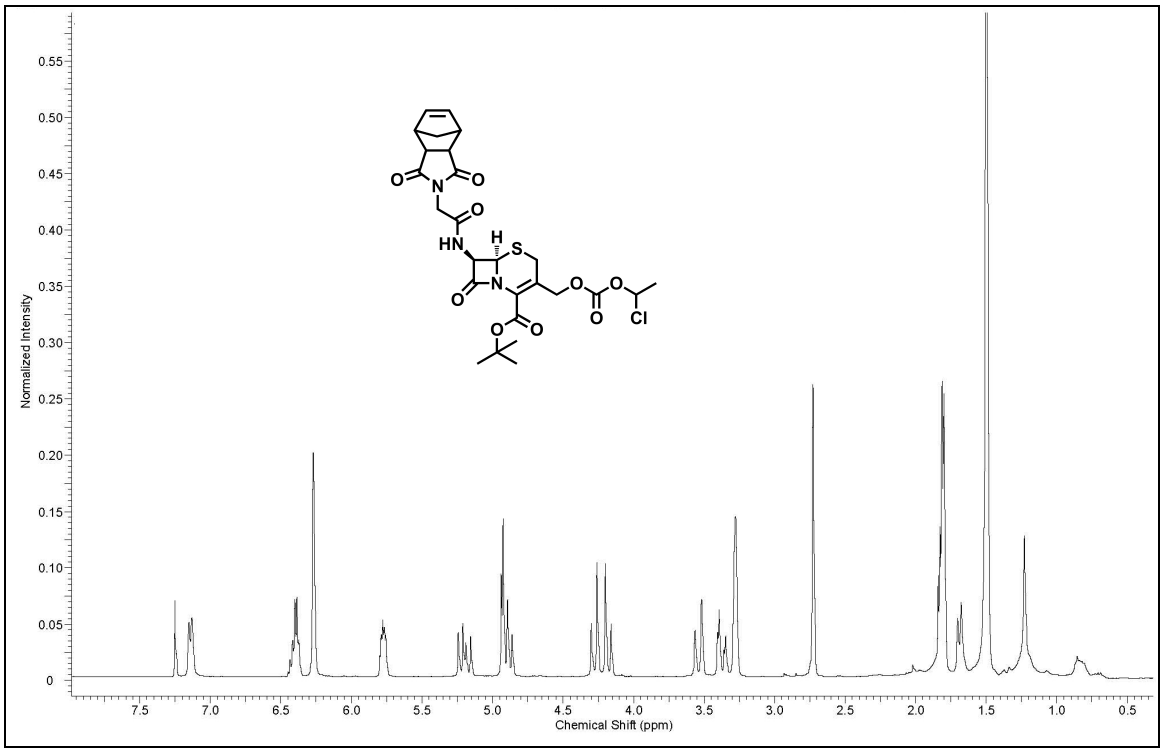

Figure 2.26: ^{1}H NMR of **10**.

(2*S*)-bicyclo[2.2.1]hept-5-ene-2-carbonyl chloride (13). To a Schlenk flask, compound **14** (57.5mg, 0.42mmol) was dissolved in dry DCM (3mL). Thionyl chloride (45.5 μL, 0.43mmol) was added drop wise over an oil bath. The reaction was refluxed for 4 hours and allowed to cool to room temperature. The solvent was removed in vacuo and a white powder was observed to obtain **13** (50.0mg, 0.32mmol, 77.00%). **Figure 2.27**: ^{1}H NMR (400MHz, $CDCl_3$): δ 1.48 (m, 4H), 2.03 (dd, 1H), 2.75 (m, 1H), 2.99 (s, 1H), 3.29 (s, 1H), 6.13 (d, 1H), 6.21 (d, 1H).

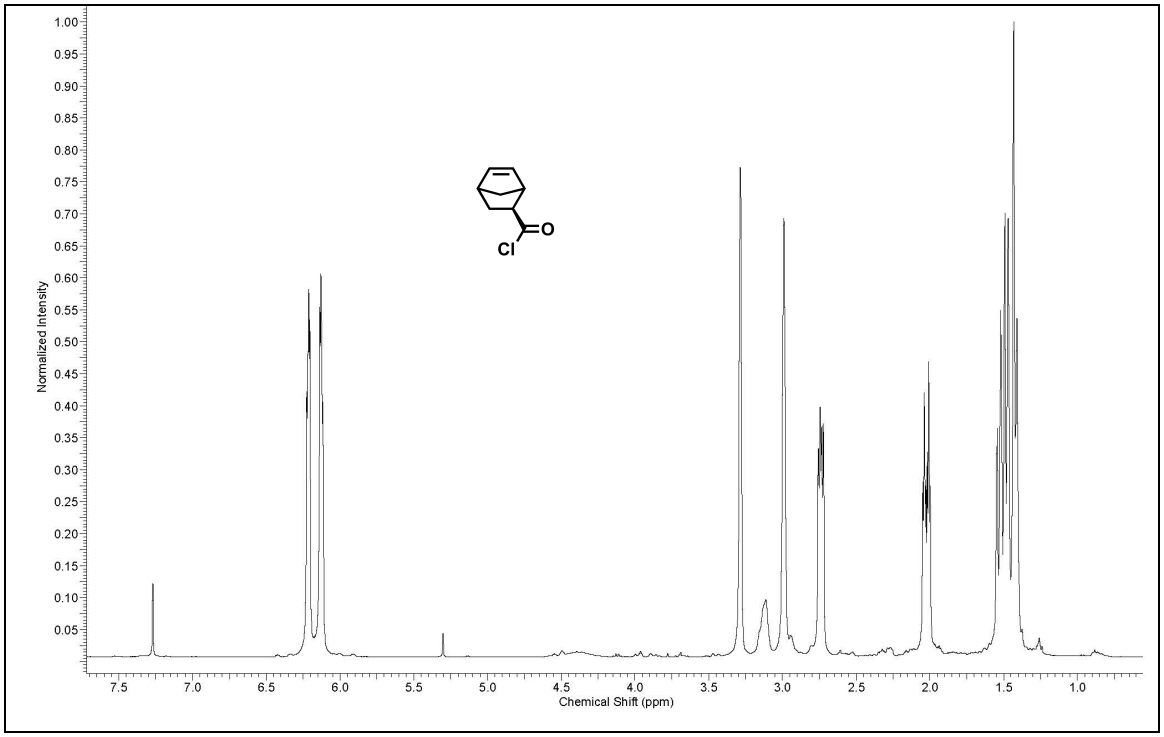

Figure 2.27: ^{1}H NMR of **13**.

1-chloroethyl (2-(1,3-dioxo-3a,4,7,7a-tetrahydro-1*H*-4,7-methanoisoindol-2(3*H*)-yl)ethyl) carbonate (17). Compound **16** (203.2mg, 0.98mmol) and 1-chloroethyl chloroformate (110μL, 1.10mmol) were dissolved in dry DCM. The reaction was cooled over an ice bath and pyridine (100μL, 1.24mmol) was added drop wise. The reaction was stirred for 1.5 hours and the reaction was diluted with dry DCM (30mL). The organic layer was washed with 0.5N HCl (10mL) and deionized water (2 x 10mL). The organic layer was dried over MgSO4, filtered, and concentrated under reduced pressure. The product was purified by flash chromatography using 2:1 EtOAc/Hexanes mixture. Compound **17** was isolated as a clear oil (245.0mg, 0.78mmol, 79.63%). R_f 0.74 (2:1 EtOAc/Hexanes);); **Figure 2.28**: ^{1}H NMR (400MHz, $CDCl_3$): δ 1.19 (d, 1H), 1.47 (d, 1H), 1.71 (d, 3H), 3.17 (s, 2H), 3.63 (s, 2H), 3.66 (m, 1H), 3.76 (m, 1H), 4.24 (m, 2H), 6.19 (s, 2H), 6.29 (q, 1H). HRMS (M+Na): calculated: 336.0609; found 336.0610.

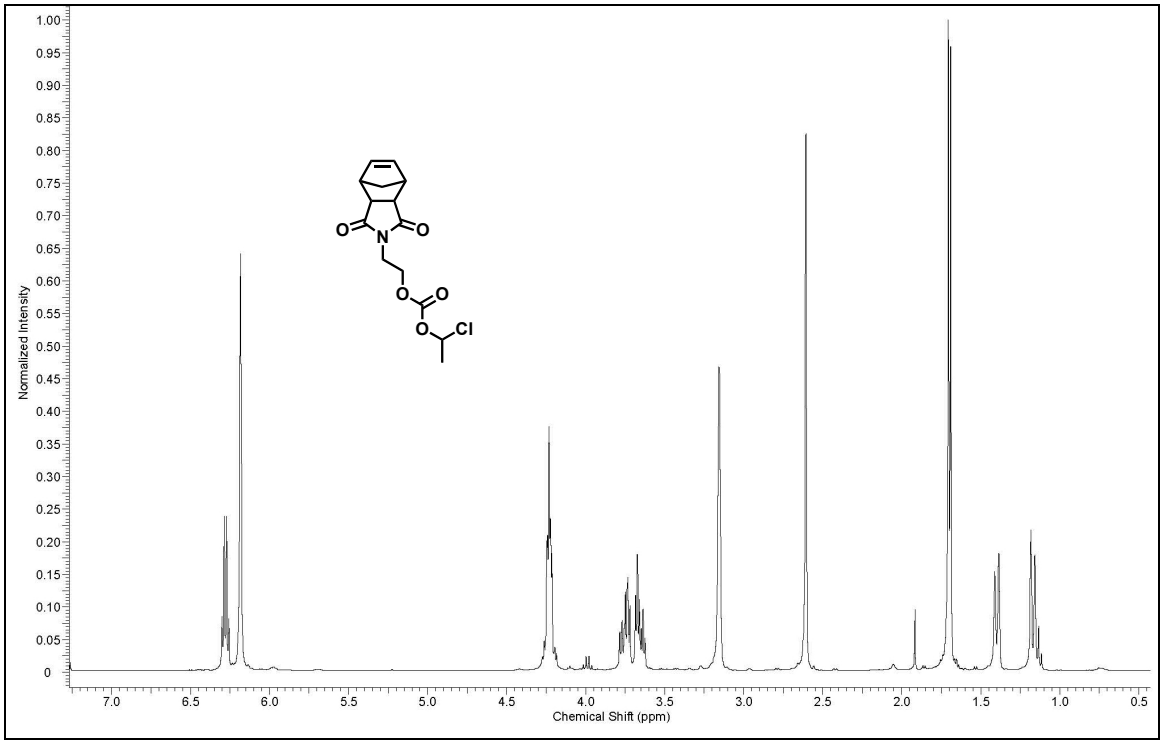

Figure 2.28: ^{1}H NMR of **17**.

2.7 – References

(1) Satchi-Fainaro, R.; Hailu, H.; Davies, J. W.; Summerford, C.; Duncan, R. *Bioconjugate Chemistry* **2003**, *14*, 797-804.

(2) Blau, L.; Menegon, R. F.; Chung, M. C. *Quimica Nova* **2006**, *29*, 1307-1317.

(3) Ouyang, M.; Huang, H.; Shaner, N. C.; Remacle, A. G.; Shiryaev, S. A.; Strongin, A. Y.; Tsien, R. Y.; Wang, Y. *Cancer Res* **2010**, *70*, 2204-12.

(4) Jiang, T.; Olson, E. S.; Nguyen, Q. T.; Roy, M.; Jennings, P. A.; Tsien, R. Y. *Proc Natl Acad Sci U S A* **2004**, *101*, 17867-72.

(5) Amir, R. J.; Zhong, S.; Pochan, D. J.; Hawker, C. J. *Journal of the American Chemical Society* **2009**, *131*, 13949-13951.

(6) Patterson, L. D.; Miller, M. J. *J Org Chem*, *75*, 1289-92.

(7) Kline, T.; Torgov, M. Y.; Mendelsohn, B. A.; Cerveny, C. G.; Senter, P. D. *Molecular Pharmaceutics* **2004**, *1*, 9-22.

(8) Lee, G. Y.; Song, J.-h.; Kim, S. Y.; Park, K.; Byun, Y. *Drug Development Research* **2006**, *67*, 438-447.

(9) Liu, S.; Netzel-Arnett, S.; Birkedal-Hansen, H.; Leppla, S. H. *Cancer Research* **2000**, *60*, 6061-6067.

(10) D'Souza, A. J. M.; Topp, E. M. *Journal of Pharmaceutical Sciences* **2004**, *93*, 1962-1979.

(11) Bareford, L. M.; Swaan, P. W. *Advanced Drug Delivery Reviews* **2007**, *59*, 748-758.

Chapter 3 – Ring-Opening Metathesis Polymerization of Stimuli-Responsive Monomers

---

3.1 – Introduction

Ring-opening metathesis polymerization (ROMP) is an easily deployed method in the synthesis of highly functionalized complex polymers and copolymers.[1-3] This living polymerization method allows for the olefin-metathesis of norbornene-based functionalized monomers.[2] The thermodynamic driving force behind the polymerization of norbornene is the release of ring strain.[2] In synthesizing polymers, we utilized Grubb's ruthenium catalyst due to its high functional group tolerance and stability in air.[2,4-8] **Figure 3.1** illustrates the general scheme for ROMP. Accordingly, ring-opening metathesis polymerization was utilized to generate polymers containing monomers **1-4**.

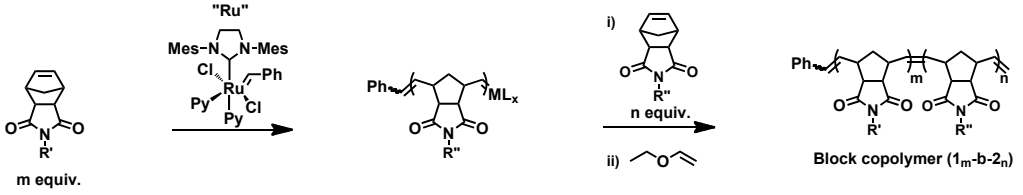

Figure 3.1: General scheme for ROMP.

In demonstrating the preparation of these stimuli-responsive polymers, we can better understand the types of functional group that the catalyst can withstand as well as the rate at which the polymerization goes to completion. The incorporation of different monomers allows the synthesis of block copolymers, which can be fully characterized.

This chapter discusses the polymerization of monomers **1-4** to better understand whether β-lactamase-responsive polymers are proficient in the assembly of micellar nanostructures.

3.2 – Polymerization of β-lactamase-Responsive Monomers

Grubb's catalyst shows high tolerance for many functional groups as well as complex and high molecular weight molecules.[5-8] However, we were uncertain whether cephalosporin-based norbornene monomers would be treated in the same fashion. Towards the development of β-lactamase-responsive materials, we aimed to synthesize and design polymers containing this class of novel monomers.

3.2.1 – Ruthenium Catalyst Tolerance of Norbornene Cephalosporin-Based Monomers

In synthesizing monomer **1**, the norbornene moiety as well as the PEG leaving group were not a concern with respect to polymerization, however the cephalosporin linker had not been successfully polymerized in the literature. Of specific concern is the fact that the cephalosporin linker contains a cyclic thioether. Therefore, we were unsure whether the catalyst would be inhibited by the functional group. To confirm the ruthenium catalyst tolerance of the cephalosporin linker, compound **8** was polymerized via ROMP to afford polymer **6**. The polymerization of **8** in **Figure 3.2** confirms that the thioether does not terminate metal catalyst activity and that the ruthenium catalyst can in fact tolerate cephalosporin-based monomers.

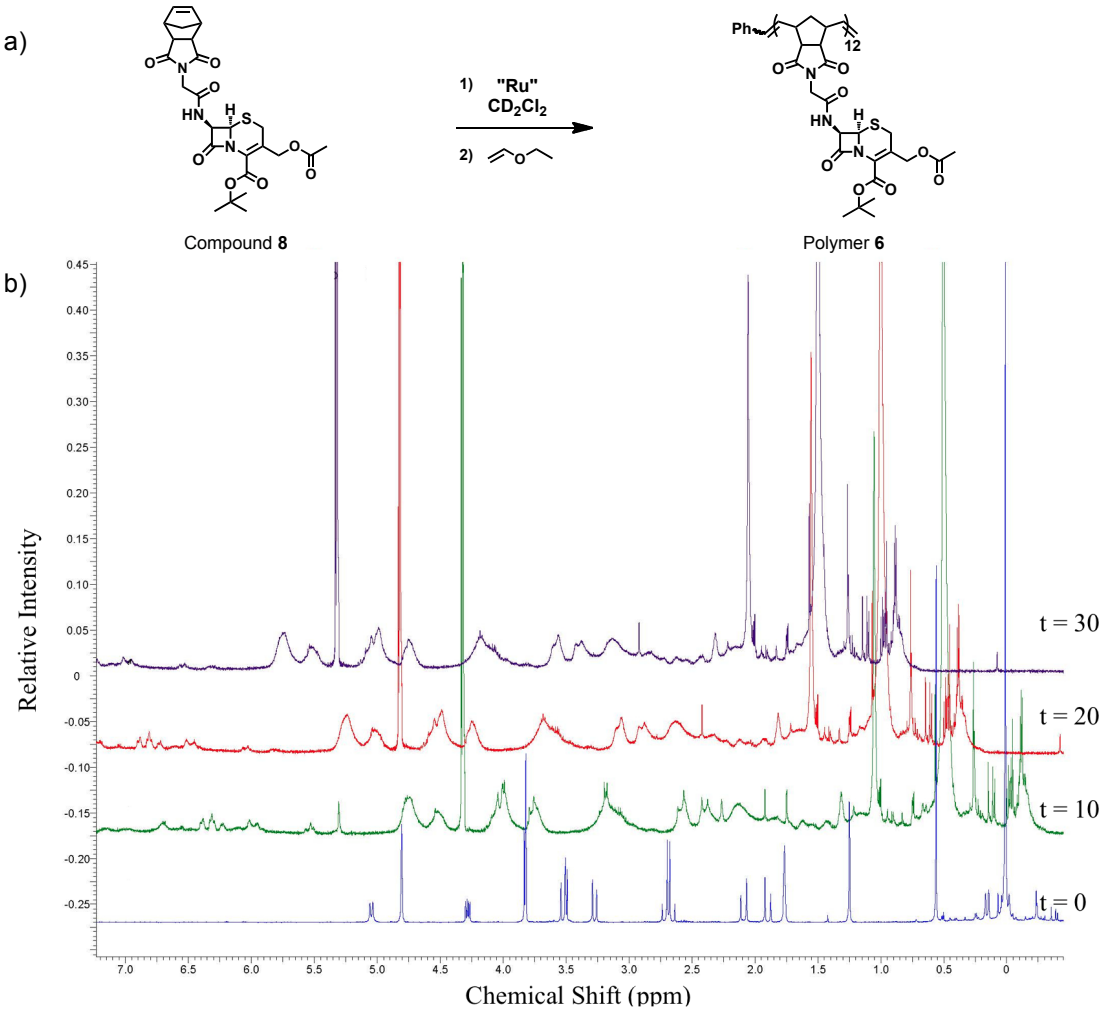

Figure 3.2: ROMP of compound **8.** a) Synthesis of polymer **6**. b) ^{1}H NMR time course analysis of **8**.

The polymerization of compound **8** was monitored by ^{1}H NMR time course analysis. The norbornene olefin resonances at 4.75 parts per million (ppm) were monitored for disappearance over time, as the norbornene was subjected to ROMP in **Figure 3.2b**. After 10 minutes, the intensity of the olefin peak had significantly decreased and by 30 minutes the peak had completely disappeared confirming the complete

consumption of **8**. Furthermore, the appearance of broad peaks confirms the formation of polymer backbone demonstrating the polymerization of compound **8** was successful. In conclusion, cephalosporin-based monomers are tolerated.

3.2.2 – Proof-of-Concept for the Formation of Micellar Nanoparticles

To determine if the cleaved product of monomer **1** is hydrophobic enough with respect to the activated amphiphile, a block copolymer was synthesized using compound **8** as a putative hydrophobic block and PEG monomer **18** as the hydrophilic block to afford polymer **2**. Compound **8** is an analog of **1**, yet it lacks a hydrophilic moiety. Consequently, **8** was polymerized in the synthesis of polymer **7** as a control test for micelle formation of an enzymatically cleaved amphiphile. The synthesis of block copolymer **7** is shown in **Figure 3.3**.

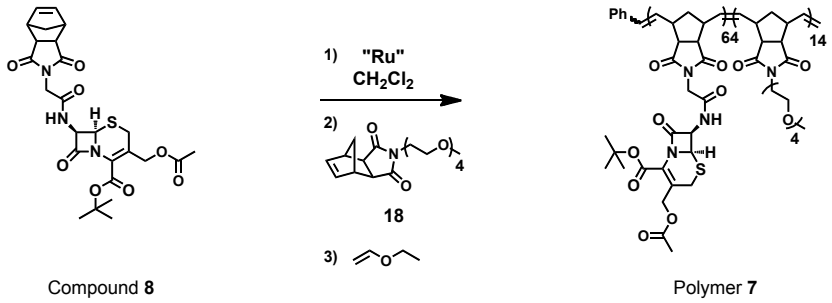

Figure 3.3: Synthesis of block copolymer **7**.

As analyzed by static light scattering (SLS), polymer **7** showed a low polydispersity (PDI) value of 1.010 and number molecular weight of M_n = 3.889 x 10^4. The theoretical ratio of compound **8** to PEG monomer **18** was 80:20, however 64:14 was

observed. Amphiphilic block copolymers containing cephalosporin-based monomers can be polymerized and characterized to afford monodispersed polymer **7**.

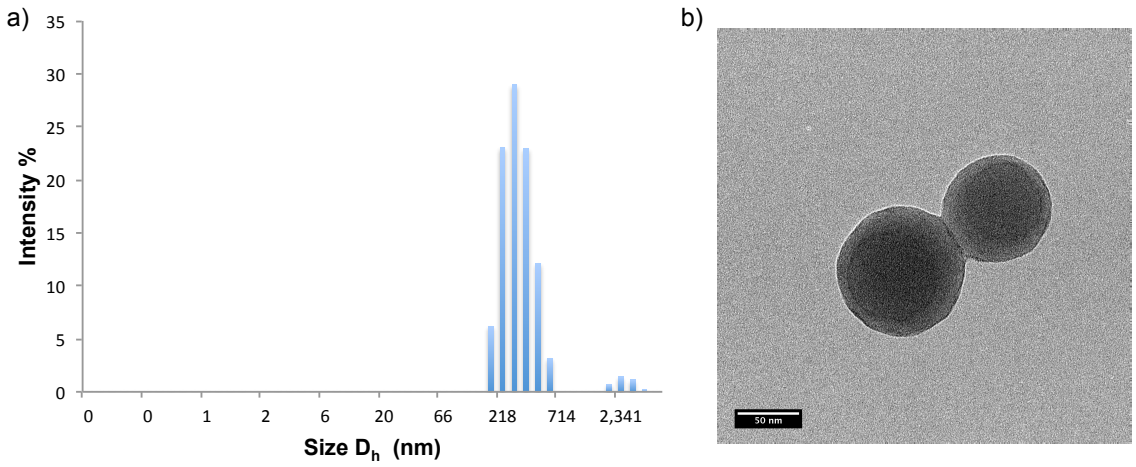

Figure 3.4: Characterization polymer 7 after dialysis. a) DLS data of polymer **7** after dialysis, b) TEM image of spherical micelles after dialysis of polymer **7**.

Polymer **7** was dialyzed into water from dimethylsulfoxide (DMSO) and micellar nanoparticles were formed. Dynamic light scattering (DLS) data suggest the majority of these particles are 300 nm in diameter. However, the transmission electron microscopy (TEM) images in **Figure 3.4** display 50 nm micelles, which is inconsistent with DSL data. Regardless of the size of the observed micelles, this control suggests that amphiphilic β -lactamase cleaved block copolymers are capable of forming micellar nanoparticles.

3.3 – Polymerization of β-lactamase-Responsive Pre-Amphiphilic Block Copolymers

In designing a β-lactamase pre-amphiphile substrate polymer, the polymer must contain an enzyme-responsive unit specific to β-lactamase enzyme. The enzyme-

responsive unit should harness hydrophilic moieties that allow the polymer to fully solubilize in water.[9] Additionally, the substrate should also be accessible for β-lactamase cleavage to activate the pre-amphiphilic polymer in becoming amphiphilic for micelle formation. To monitor the self-assembly, the polymers are dye-labeled at the hydrophilic end with fluorescein and rhodamine termination agents. Specifically, when enzymatically activated, the complementary dye-labeled polymers assemble to provide a handle on particle formation via fluorescence resonance energy transfer as illustrated in **Figure 3.5**. Herein, the synthesis and design of the dye-labeled β-lactamase pre-amphiphile polymer is described.

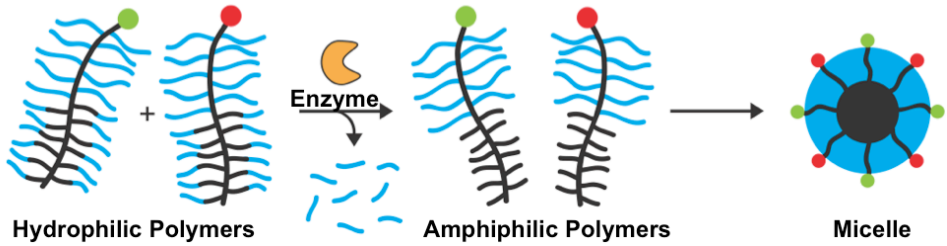

Figure 3.5: General scheme for the enzyme-directed assembly of dye-labeled micellar nanoparticles.

3.3.1 Designing Pre-Amphiphilic Block Polymers

Polymers $\mathbf{1_F}$-$\mathbf{5_R}$ were synthesized via ROMP using Grubb's modified 2nd generation ruthenium catalyst. The polymerization of monomer **1** served as the β-lactamase-responsive block (n), followed by one of two different PEG monomers as the fully hydrophobic block (m). The polymer solution mixtures were split and quenched with either fluorescein or rhodamine termination agents as outlined in **Figure 3.6**.

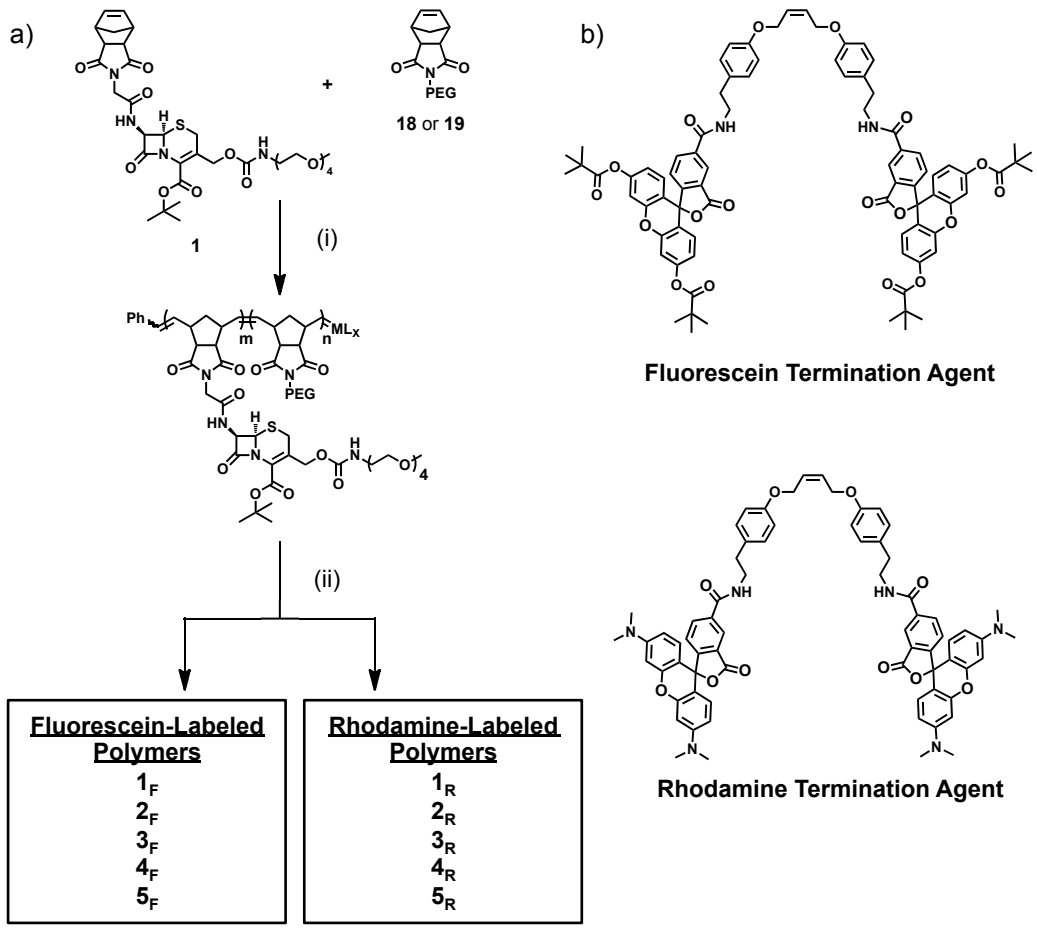

Figure 3.6: Synthesis of polymers **1-5**. a) General synthetic scheme. (i) Polymerization of monomer **1** with either PEG **18** or **19**. (ii) Splitting and quenching of polymers with either fluorescein or rhodamine termination agents. b) Structures of fluorescein and rhodamine termination agents.

Figure 3.7: General structure of polymers **1-5**. a) Structure of polymers **1-5**. b) Fluorescein and rhodamine dyes.

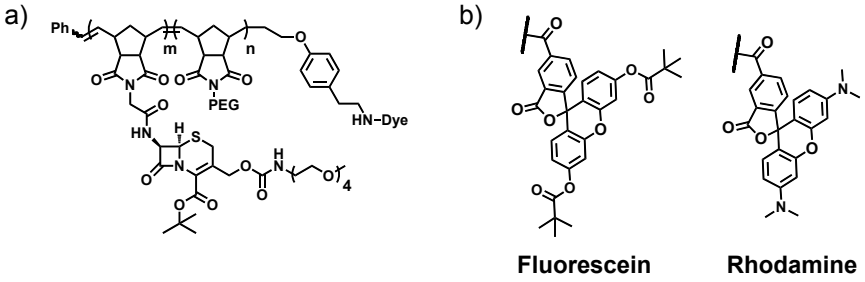

Table 3.1: β-lactamase-responsive pre-amphiphilic block copolymers.

Polymers	m	n	Mn	Mn/Mz (PDI)	Conditions	Radius (nm)
1_F	n/a	n/a	2.762×10^4	1.071	ABE	59.8
1_R	n/a	n/a	2.994×10^4	1.040	ABE	0.3
2_F	n/a	n/a	1.150×10^4	1.012	AB	0.41
2_R	n/a	n/a	9.761×10^3	1.040	AB	n/a
3_F	27	n/a	1.238×10^4	1.055	AB	35.0
3_R	27	n/a	1.517×10^4	1.486	AB	27.4
4_F	9	47	2.416×10^4	1.005	AB	34.1
4_R	9	47	2.361×10^4	1.004	AB	27.4
5_F	20	32	3.516×10^4	1.033	CDE	52.7
5_R	20	32	3.595×10^4	1.024	CDE	39.6

A) Dialyzed from DMSO into H_20 at 0.5mg/mL; B) PEG Monomer **18**;
C) Dialyzed from MeOH into H_20 at 2.0mg/mL; D) PEG Monomer **19**;
E) Polymerized inside glove box. F = Fluorescein labeled, R = Rhodamine labeled.

Polymers $\mathbf{1_F}$-$\mathbf{5_R}$ were analyzed by SLS. During polymer synthesis, a sample of each polymerization block was quenched with ethyl vinyl ether and measured for block length. Block lengths of polymers $\mathbf{1_F}$-$\mathbf{2_R}$ could not be accounted for due to the failure of obtaining reaction sample for the full characterization by SLS. A lower value of average molecular weight was reported for polymers $\mathbf{3_F}$ and $\mathbf{3_R}$, which explains the absence of data for the hydrophilic (n) block. All polymers with the exception of $\mathbf{3_R}$ displayed low

polydispersity index values indicating monodispersed polymers. The polymerization of monomer **1** and synthesis of polymers $\mathbf{1_F}$-$\mathbf{5_R}$ provides evidence of the viability of this method towards generating enzyme-responsive polymeric micelles.

3.3.2 – Solvent Effects on Aggregation

Polymers $\mathbf{1_F}$-$\mathbf{5_R}$ were dialyzed from organic solvent (either DMSO or MeOH) into water and measured by dynamic light scattering. Polymers $\mathbf{1_R}$, $\mathbf{2_F}$, and $\mathbf{2_R}$ did not form aggregates in solution. The remaining polymers exhibited aggregated material ranging from 27.4nm to 59.8nm in radius. The result of aggregation may be a result of the hydrophobic fluorescein and rhodamine dyes. Due to the high sensitivity of DLS, the data may be an inaccurate representation of the formation of a few particles that have formed in aqueous solution. Polymers $\mathbf{1_F}$ and $\mathbf{3_F}$-$\mathbf{5_R}$ may in fact be free unaggregated polymers; however experiments should be further explored. Serial dilutions of polymer $\mathbf{5_F}$ and $\mathbf{5_R}$ in magnesium chloride were aimed at breaking up the ionic characteristics of the dyes; however measurements indicated aggregates even in salt solution.

The data from DLS suggests that these polymers regardless of initial organic solvent form aggregates upon addition and dialysis into deionized water. The aggregation of polymers in aqueous solution creates a problem for the overall goal of the project, as the formation of nanoparticles should be the result of enzyme hydrolysis and not through solvent exchange. Furthermore, the cluster of polymers creates another concern about substrate accessibility for the enzyme active site. As these polymers assemble, the β-lactamase may not gain access towards the enzyme substrate, which may accumulate in the core of these aggregates. Without docking to the substrate, the activity of β-lactamase

will not be possible. Instead of dialyzing into water, the polymers should be dialyzed into the appropriate reaction buffer corresponding to the enzyme reaction conditions. These polymers will ultimately be digested with enzymes. Therefore it only seems logical to dialyze these materials into the reaction buffer as the material may behave differently in salt solution.

3.4 – Attempted Polymerization of Disease-Associated Protease Peptide Substrate Monomer

Diseased-associated tissues are known to overexpress certain proteases at the cell surface as well as the ECM.[10-12] Exploiting these endogenously expressed proteases, we aim to present peptide substrate polymeric materials that undergo a selective and specific targeting of diseased cells. To prepare such materials that serve as a molecular diagnostic for disease detection and drug release, peptide substrate monomers must first be capable of ring-opening metathesis polymerization. Herein, we describe the efforts towards the polymerization of peptide monomers substrates.

We attempted to polymerize monomer **3** via ROMP. To investigate whether the ruthenium catalyst would tolerate the functional groups of the dye-labeled diseased-associated peptide substrate monomer, ^{1}H NMR time course analysis was employed to monitor the reaction. Using a deuterated solvent mixture of 2:1 CD_2Cl_2/MeOH, monomer **3** was unable to solubilize in the solution. Monomer **3** requires a much more polar solvent system, in which the substrate monomer is able to fully dissolve in pure methanol. Increasing the ratio of methanol in the CD_2Cl_2/MeOH mixture precipitated out the

catalyst. As a result, in order to polymerize monomer **3**, a polar solvent system that is tolerated by ruthenium catalyst must be explored.

In considering the use of different solvents, the polymerization of **3** should be attempted in deuterated DMF to monitor the living polymerization. Particularly, our lab has polymerized various different peptide monomers using DMF as solvent. Although DMF may alleviate the solubility issue of monomer **3**, the functional groups from the peptide side chains may also potentially inhibit the catalyst from polymerizing. To confirm the polymerization of **3**, deuterated DMF including various solvent systems if necessary, should be explored in the presence of Grubb's ruthenium catalyst. Due to solubility issues, the polymerization of **3** cannot be confirmed at the present moment.

3.5 – Polymerization of Acid Labile Doxorubicin Prodrug Monomer

In developing enzyme-responsive prodrug polymeric materials, we aimed to synthesize polymers responsive to various stimuli as the control experiment in contrast to enzyme-responsive polymers. For this reason, the polymerization of monomer **4** is described.

Using ruthenium catalyst, monomer **4** was polymerized via ROMP as shown in **Figure 3.8**. The polymerization was monitored in real time over ^{1}H NMR time course analysis. The data was referenced to deuterated DCM and the norbornene olefins of monomer **4** are observed at 5.85 ppm. After the addition of catalyst, the intensity of the olefins significantly decreased at t =10 minutes. At t = 30 minutes, the olefins completely disappear confirming the full completion of polymerization. The appearance of a broad

peak at 5.0 ppm suggests the formation of polymer backbone. Thus, ^{1}H NMR time course analysis shows the quick and efficient polymerization of **4** to afford polymer **8**.

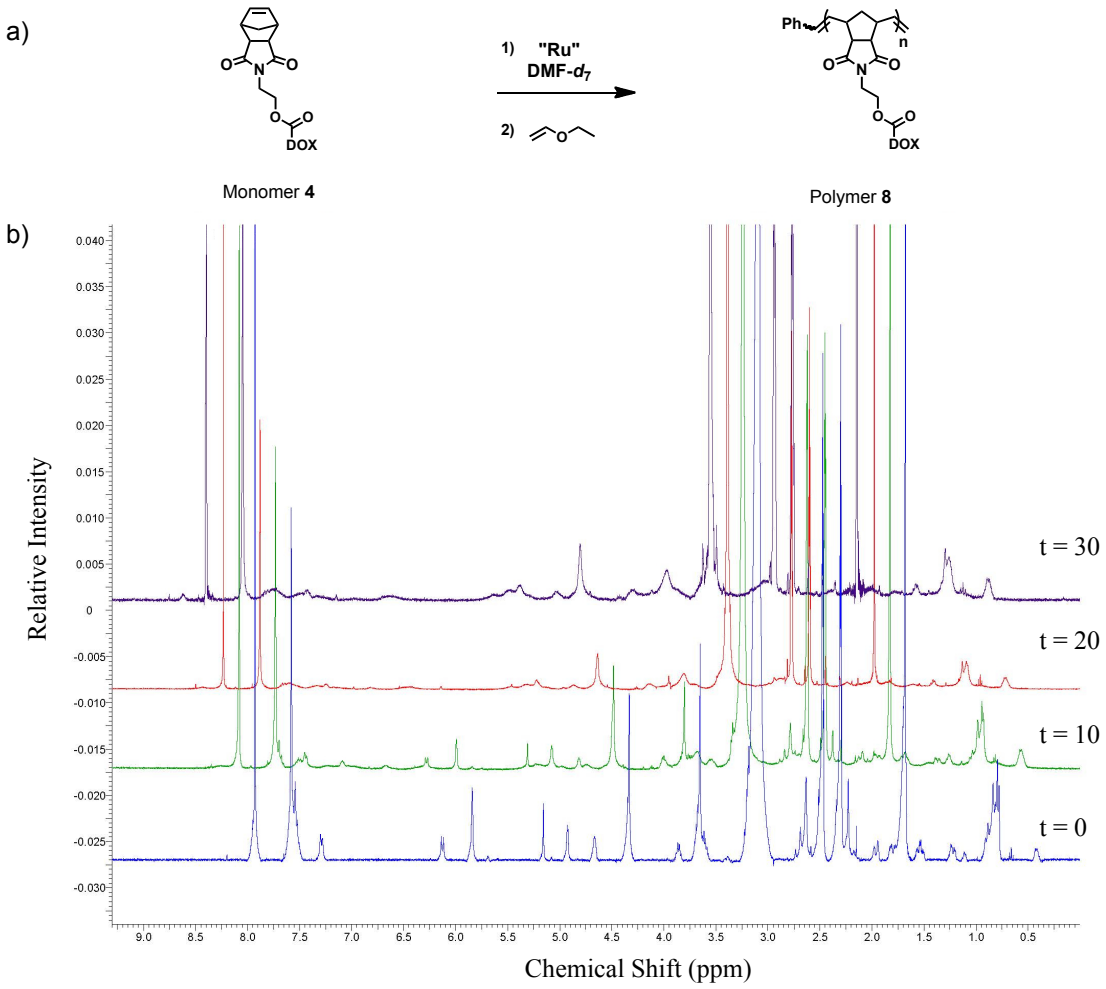

Figure 3.8: a) Synthesis of polymer **8**. b) ^{1}H NMR time course analysis of monomer **2**.

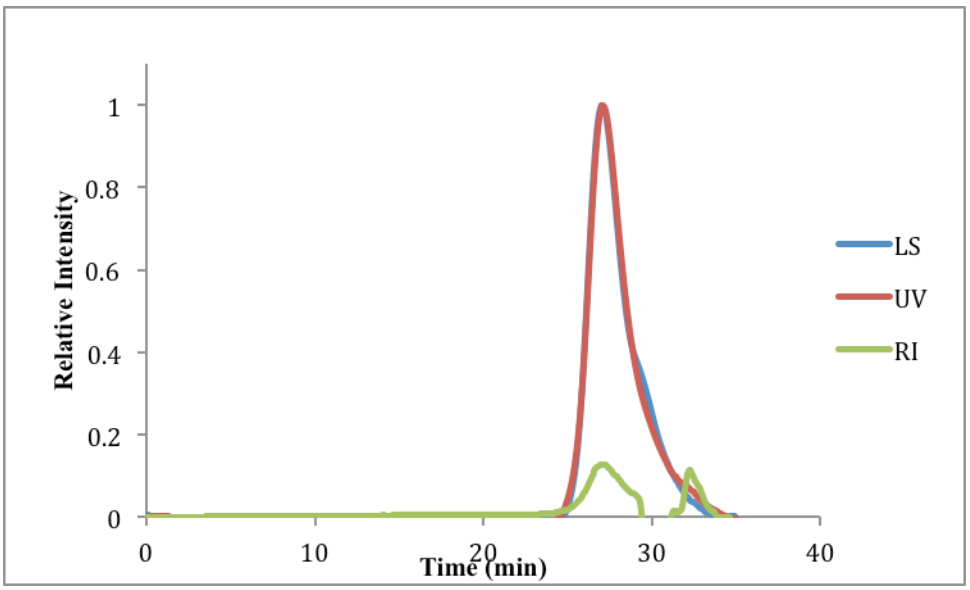

Figure 3.9: SLS characterization of polymer **8**. LS = Light scattering, UV = Ultraviolet , RI = Refractive index.

Polymer **8** was characterized by SLS as shown in **Figure 3.9**. Data shows an excellent light scattering signal however the data is not an accurate representation of the homopolymer. Doxorubicin absorbs near the wavelength of the instrument detector, which explains the inaccurate value for M_n. The reported value for $M_n = 4.819 \times 10^5$ suggest that the polymer is extremely large, however due to the long retention time (27 mins) in comparison to polymers **1-5**, homopolymer **8** is actually lower in molecular weight.

From this, polymers exhibiting low polydispersity containing monomer **4** can be easily polymerized and monitored by ^{1}H NMR time course analysis. Doxorubicin can be incorporated within these polymeric systems however, the spectroscopic nature of the drug causes problems for characterization by SLS. Further experiments should be

conducted using a detector that will not be interfered with by the fluorescent nature of doxorubicin. Proper data would allow for the full characterization of the polymer **8** in terms of molecular weight and repeating monomer units.

3.6 – Conclusions

In this chapter, we have shown that monomers **1**, **4** and compound **7** are capable of ROMP. However, the polymerization of monomer **3** has yet to be confirmed due to solubility issues. All ^{1}H NMR time course analysis of these monomers shows the polymerization to be relatively fast and efficient. In conjunction with previous reports, Grubb's modified catalyst demonstrates high functional group tolerance. This chapter specifically shows that ruthenium catalyst is tolerant to cephalosporin-based and doxorubicin monomers. Furthermore, polymers, **1-8** can be fully characterized by SLS with the exception of polymers containing fluorescent doxorubicin monomer **4**. In characterizing polymers **1-8**, all polymers display a low PDI value indicating polydispersed polymers with the exception of polymer $\mathbf{3_R}$. Despite the aggregation of polymers **1-5** in solution, dialysis of polymer **7** shows that β-lactamase-responsive polymers are capable of forming spherical micelles. The micelle formation of polymer **2** further supports the idea behind enzyme-directed assembly of micellar nanoparticles. Thus, the polymerizations of compounds **1**, **4**, and **7** all show that stimuli-responsive monomers can be polymerized for the potential application of polymer self-assembly and prodrug therapy.

3.7. Experimental

3.7.1. General Methods/Instrument Details

Anhydrous solvents were used and all solvents were degassed via nitrogen purge prior to use. Deuterated solvents were purchased from Cambridge Isotope Laboratories Inc. Deuterated methylene chloride and methanol were dried over calcium hydride, distilled, and freeze-thawed-pump degassed. Non-deuterated methylene chloride was dried using Dow-Grubbs two-column purification system (Classcontour System, Irvine, CA). All polymerizations were either carried out under dinitrogen atmosphere using standard Schlenk techniques or a Plas Labs bench top glove box unless otherwise indicated. Polymer polydispersity and molecular weight were determined by size-exclusion chromatography (Phenomenex Phenogel 5u 10, 1K-75K, 300 x 7.80mm (0.05M LiBr in DMF)) using a Hitachi-Elite LaChrom L-230 pump equipped with a multi-angle light scattering (MALS) detector (DAWN-HELIOS: Wyatt Technology) and a refractive index detector (Hitachi L-2490) normalized to a 30,000 g/mol polystyrene standard. D_h was determined by DLS on a DynaStarPro Nanostar provided byWyatt Technologies. Prior to DLS measurements, samples were filtered using 1.0 μm pore size 13 mm diameter PTFE Filter Media with Polypropylene Housing. All ^{1}H NMR spectra were recorded on Varian Mercury 300Mhz, or 400 Mhz, spectrometers. Chemical shifts are indicated in δ values (ppm) from internal reference peaks of $CDCl_3$, CD_2Cl_2, CD_3OD, or DMF-d_7. The Mass Spectrometry Facility at the UCSD Department of Chemistry and Biochemistry using Agilent 6230 HR-ESI-TOF MS provided Mass spectra.

3.7.2. General Polymer Synthesis

To a stirred solution of 1 (80 mg, 0.315 mmol) in dry CH_2Cl_2 (2 mL) was added a solution of catalyst ($(IMesH_2)(C_5H_5N)_2(Cl)_2Ru=CHPh$) (6.03 mg, 0.00829) in dry CH_2CL_2 (2 mL) . The reaction was stired for 30 minutes and a 20 μL aliquot was removed and quenched with ethyl vinyl ether. PEG was added to the remaining reaction mixture and stirred for another 30 minutes. A 20 μL aliquot was removed and quenched with ethyl vinyl ether. The remaining reaction mixture was split and separately quenched with fluorescein and rhodamine termination agents. All quenched aliquots were precipitated in cold ether, centrifuged, and the ether was removed to afford a solid. All samples were analyzed by SEC-MALS to obtain block length, molecular weight, and polydispersity. Data provided in **Table 3.1**.

3.7.3. Dialysis

Polymer samples were dissolved in either DMSO or MeOH followed by the addition of equal volume of water. Ammonium hydroxide (20 μL) was added to the polymer solutions labeled with fluorescein to deprotect the dye. These solutions were then transferred to a 3,500 MWCO Snakeskin dialysis tubing and dialyzed into water. After 24 hours, the solutions were transferred to a 10,000 MWCO Snakeskin dialysis tubing and dialyzed for another 2-3 days. Water was changed daily.

3.8 – References

(1) Carrillo, A.; Kane, R. S. *Journal of Polymer Science, Part A: Polymer Chemistry* **2004**, *42*, 3352-3359.

(2) Sanford, M. S.; Love, J. A.; Grubbs, R. H. *Journal of the American Chemical Society* **2001**, *123*, 6543-6554.

(3) Ilker, M. F.; Schule, H.; Coughlin, E. B. *Polymer Preprints (American Chemical Society, Division of Polymer Chemistry)* **2003**, *44*, 659-660.

(4) Furstner, A. *Angewandte Chemie, International Edition* **2000**, *39*, 3012-3043.

(5) Fraser, C.; Grubbs, R. H. *Macromolecules* **1995**, *28*, 7248-55.

(6) Weck, M.; Schwab, P.; Grubbs, R. H. *Macromolecules* **1996**, *29*, 1789-93.

(7) Strong, L. E.; Kiessling, L. L. *Journal of the American Chemical Society* **1999**, *121*, 6193-6196.

(8) Bertin, P. A.; Smith, D.; Nguyen, S. T. *Chemical Communications (Cambridge, United Kingdom)* **2005**, 3793-3795.

(9) Amir, R. J.; Zhong, S.; Pochan, D. J.; Hawker, C. J. *Journal of the American Chemical Society* **2009**, *131*, 13949-13951.

(10) Kline, T.; Torgov, M. Y.; Mendelsohn, B. A.; Cerveny, C. G.; Senter, P. D. *Molecular Pharmaceutics* **2004**, *1*, 9-22.

(11) Lee, G. Y.; Song, J.-h.; Kim, S. Y.; Park, K.; Byun, Y. *Drug Development Research* **2006**, *67*, 438-447.

(12) Liu, S.; Netzel-Arnett, S.; Birkedal-Hansen, H.; Leppla, S. H. *Cancer Research* **2000**, *60*, 6061-6067.

Chapter 4 – Triggering of β-lactamase-Responsive Polymeric Materials

4.1 – Introduction

The assembly of amphiphilic block copolymers into defined 3-dimensional architectures has prompted an interest towards implementing responsive functionality within these polymers. Exploiting the intrinsic properties of amphiphilic polymers, the formation and manipulation of supramolecular nanostructures can be elicited by an external stimulus. Such stimuli have included pH, temperature, light, and solvent.[1-4] Although the development of amphiphilic polymers has been explored with a wide range of stimuli, there remains a lack of progression towards enzyme-directed assembly and indeed biochemically driven assembly in general.[5] This chapter attempts to address the role of β-lactamase in the cleavage of cephalosporin-based pre-amphiphilic polymers as well as introducing acidic environments for the self-assembly of micellar nanoparticles. Here, we describe the triggering of β-lactamase-responsive monomer **1** and β-lactamase pre-amphiphilic polymers $\mathbf{5_F}$ & $\mathbf{5_R}$.

4.2 – Acid Hydrolysis of β-lactamase-Responsive Polymeric Materials

As an initial step towards studying β-lactamase-directed assembly, we averted our attention to prove whether the remnants of cleaved polymer could form micellar nanoparticles. As mentioned before, carbamates are prone to hydrolysis under acidic conditions releasing carbon dioxide and the attached leaving group.[6] Therefore, cephalosporin-based polymers $\mathbf{5_F}$ and $\mathbf{5_R}$ were treated with phosphoric acid (H_3PO_4) for

the formation of micellar nanoparticles as a control experiment. The reaction conditions for the treatment of acid are provided in **Table 4.1**.

Table 4.1: H_3PO_4 treatment of polymers $\mathbf{5_F}$ and $\mathbf{5_R}$.

Entry	Polymer	Solution	Observation
1		MeOH	-
2	5_F	MeOH + H_3PO_4	Micelles
3		Water + H_3PO_4	Aggregation
4		MeOH	-
5	5_R	MeOH + H_3PO_4	n/a
6		Water + H_3PO_4	n/a

Under varying conditions, polymers $\mathbf{5_F}$ and $\mathbf{5_R}$ were treated with phosphoric acid and sonicated over a period of time. Polymers dissolved in methanol served as controls in the absence of phosphoric acid, labeled entry 1 & 4. Entry 2 & 5 describe polymers in methanol treated with phosphoric acid. Water dialyzed polymers incubated with acid correspond to entry 3 & 6. After treatment of polymers with acid, the solution mixtures were analyzed by ESI-MS to check for the presence of free PEG-amine. Mass spectrometry results confirm the presence of cleaved PEG disassociated from the cephalosporin linker in solution for all samples. However, because free PEG-amine was detected in the controls, this suggests PEG was released before the addition of phosphoric acid, to some degree. We rationalized that the protic solvent (methanol) may be responsible for the carbamate cleavage, however this cannot be conclusively confirmed

because the detection of PEG-amine may be an artifact as a result of the way the polymer ionizes and is fragmented.

To determine whether protic solvent truly triggers the self-assembly of micelles, polymers $\mathbf{5_R}$ and $\mathbf{5_F}$ should be analyzed in presence of various protic and aprotic solvents. These samples should further be examined by TEM and mass spectrometry. Studying the effects of various solvents on these polymeric systems would assist in confirming PEG cleavage and the assembly of micellar nanoparticles. Thus, we could not solely rely on data obtained from polymers $\mathbf{5_R}$ and $\mathbf{5_F}$ in purely methanol for the cleavage of PEG.

Additionally, the solution mixtures were analyzed by TEM. Entries 5 & 6 have yet to be examined by TEM. Entries 1 & 4 show images of what may possibly be 500 nm high-density micellar nanoparticles, however data from DLS does not supplement the observed images. Both pieces of data do not provide convincing evidence for spherical micelles. In contrast, TEM images of entry 2 in **Figure 4.1a** confirm the formation of monodisperse micellar nanoparticles. These monodisperse particles are consistent throughout the sample, however there are groups of particles bunched together. In comparison, entry 3 mainly displays clusters of aggregates throughout the sample in **Figure 4.1b**. It is uncertain whether images of entry 3 are a result of dialysis or induced by acid exposure. TEM images of dialyzed polymer $\mathbf{5_F}$ should be obtained without phosphoric acid incubation to compare with entry 3. As another control, TEM images should also be obtained with the aqueous phosphoric acid solution without polymer to observe whether the acid is responsible for the images obtained in entry 3. From the data provided at the moment, images obtained from entries 1, 3, and 4 do not convincingly

confirm monodispersed micellar nanoparticles, however entry 2 exhibits such nanostructures.

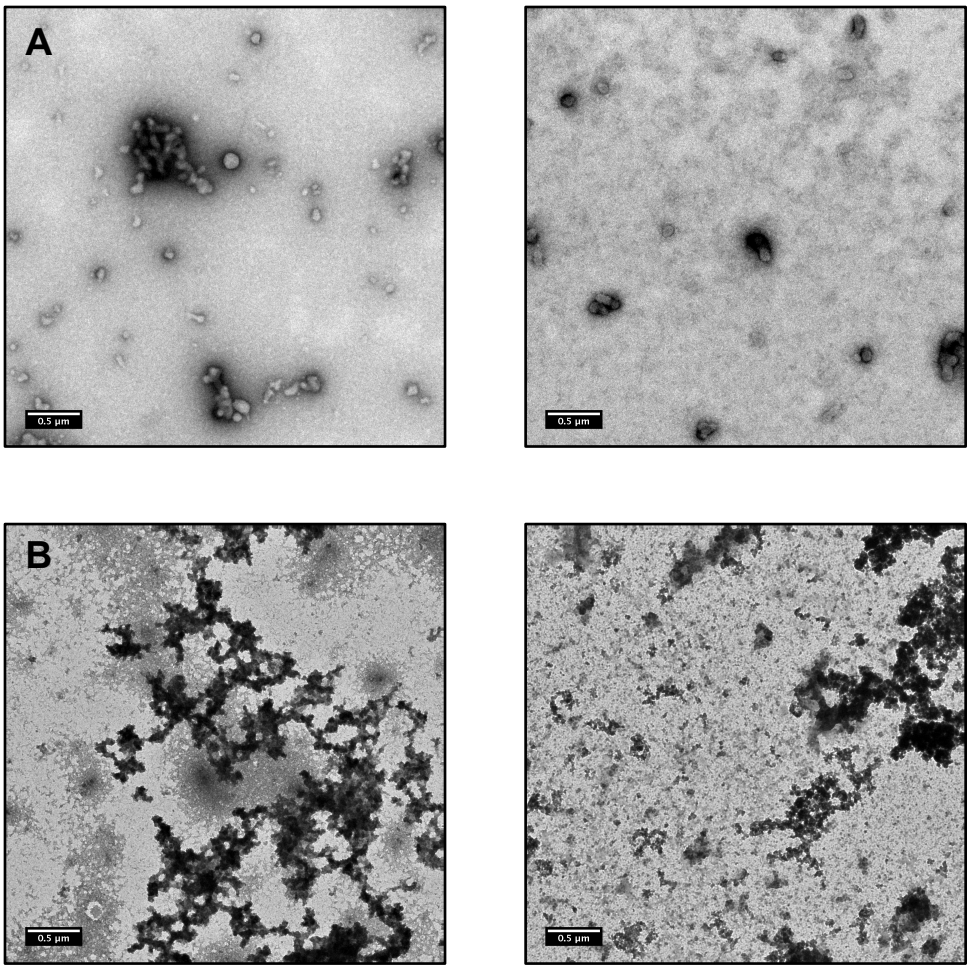

Figures 4.1: TEM images of polymers $\mathbf{5_F}$ & $\mathbf{5_R}$ treated with phosphoric acid. (A) Entry 2. (B) Entry 3.

From these studies, polymers $\mathbf{5_R}$ and $\mathbf{5_F}$ may be susceptible to carbamate cleavage in methanol, however this is yet to be determined. Further studies should be carried out using various polar and aprotic solvents. Consequently, the formation of micellar

nanoparticles from polymers $\mathbf{5_R}$ and $\mathbf{5_F}$ is only apparent in entry 2. It is highly unlikely particles are present in entry 1 & 4, and more controls are needed for entry 3 & 6.

Thus, through entry 2, we further show the proof-of-concept that β-lactamase-responsive polymers can form nanostructures upon the cleavage of PEG.

4.3 – Attempted Cleavage of β-lactamase-Responsive Monomer

As the eventual goal is the use of enzymes, specifically β-lactamase, in the assembly of polymeric materials, cephalosporin-based monomers must first show that the enzyme can cleave the substrate. In proving the cleavage of the cephalosporin substrate, we can better understand the enzyme activity and mechanism. β-lactamase can then be introduced with β-lactamase-responsive polymers to demonstrate the overall aim of the project. **Figure 4.2** illustrates the cleavage of monomer **1** via β-lactamase activity.

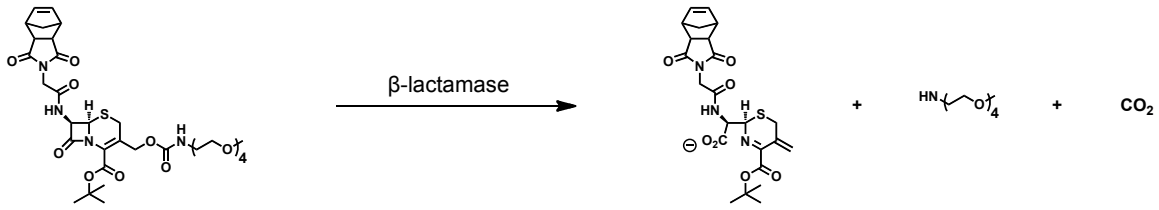

Figure 4.2: β-lactamase hydrolysis of monomer **1** to release PEG and carbon dioxide.

Two types of β-lactamases were used in the experiments described. Monomer **1** was separately incubated with penicillinase from *Bacillus cereus* and TEM-1 β-lactamase at various substrate concentrations. Enzyme reaction conditions were carried out in Tris•HCl buffer (0.1M Tris•HCl/0.1%BSA at pH 7.0) for penicillinase and phosphate buffer saline (PBS) (0.1M PBS pH 7.1) for TEM-1 β-lactamase. The reaction mixtures

were analyzed by HPLC to confirm enzyme activity. Substrate Monomer **1** in buffer solution without any enzyme was used as the control. Peaks were collected and analyzed by ESI-MS.

Table 4.2: β-lactamase reaction conditions.

Entry	Enzyme	[Enzyme] μM	[Substrate] μM
1	TEM-1 β-lactamase	-	1.0
2		0.02	1.0
3		-	10.0
4		0.02	10.0
5	penicillinase	-	2.0
6		2.0	2.0
7		-	10.0
8		10.0	10.0

Figure 4.3 shows the HPLC trace of both β-lactamase reactions at different substrate concentrations. At 7.4 minutes, a large peak was observed throughout all traces of the both enzyme reactions including the controls. A change in the peak intensity showed initial promise, however mass spectrometry does not confirm the presence of substrate monomer **1**. That peak was confirmed to be DMSO that was used initially to dissolve monomer **1**. The sharp peak near 12 minutes in all traces is a solvent peak, which is a result of the gradient steep gradient of 0-85% buffer B over 30 minutes.

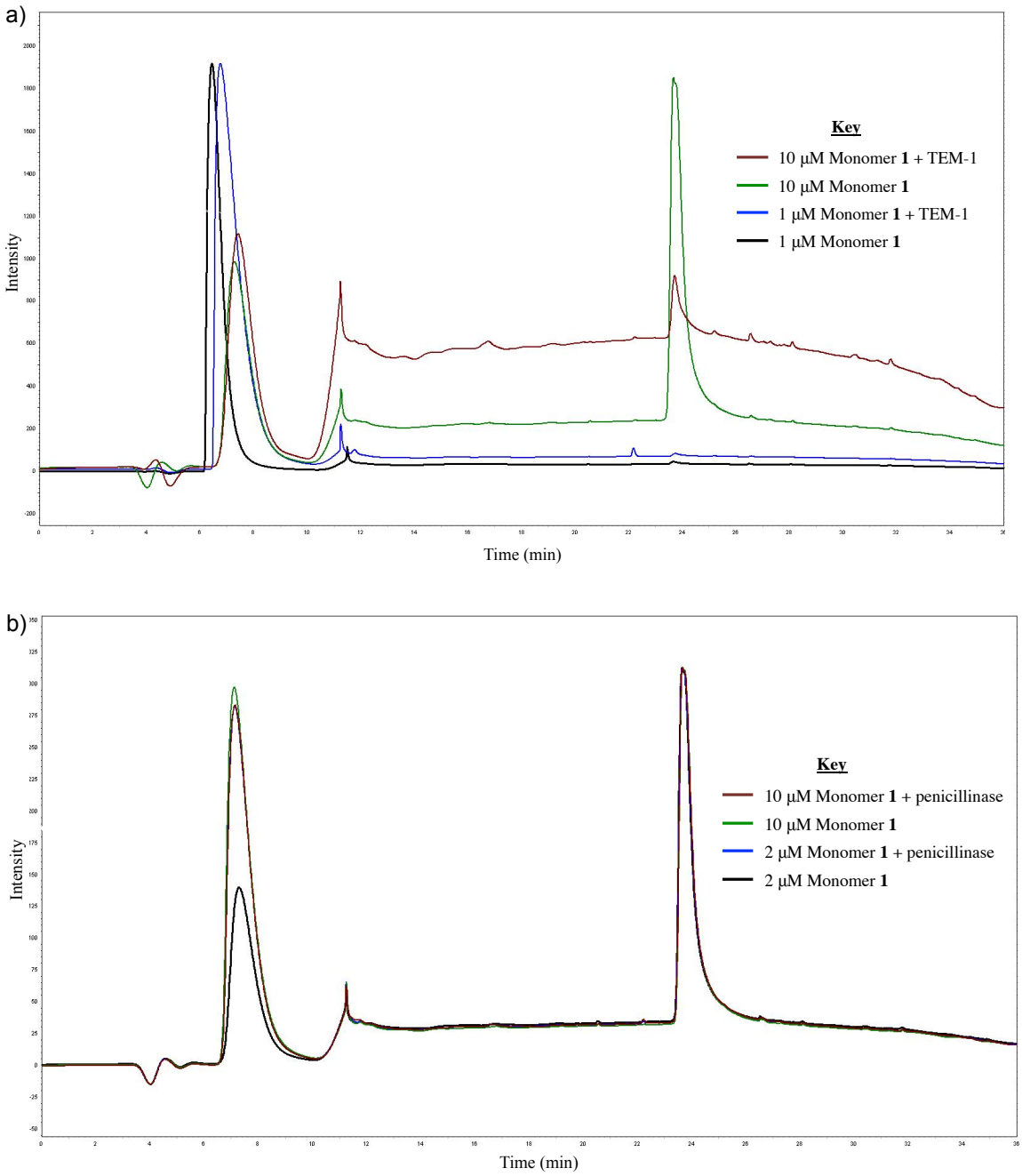

Figure 4.3: HPLC traces of β-lactamase reactions. a) TEM-1 β-lactamase reactions at various substrate concentrations in PBS buffer solution. b) Penicillinase in Tris•HCl buffer solution.

The peak at 24 minutes is observed in all traces with the exception of TEM-1 reactions at 1μM substrate concentrations. We are unsure of why the peak at 24 minutes is not apparent in those two analytical traces. A possible explanation may be a result of such low substrate concentration. Surprisingly, there is a decrease in peak intensity at that retention time in the trials that contained 10 μM substrate concentrations. The decrease in peak intensity at 24 minutes presumably demonstrates substrate cleavage of **1**. However, data obtained from mass spectrometry does not confirm the peak to be any identifiable mass. Because that peak is observed at the same intensity through all penicillin reaction traces, we do not believe that peak represents monomer **1**. The peak may possibly be a solvent peak for the Tris buffer, however we cannot explain for the appearance in the TEM-1 traces at 10μM. Ultimately, at low substrate concentrations, these experiments were limited by the course detection by the purification system. Enzyme reactions should carried out at higher substrate concentrations for the detection by HPLC.

Concerns for the design of monomer **1** became an issue due to the tert-butyl protecting group of the carboxylic acid. The steric hindrance and bulk of the protecting group may possibly interfere with the active site of β-lactamase. The inability for β-lactamase to bind to monomer **1** restricts the enzyme from cleaving the cephalosporin. To account the protected carboxylic acid for β-lactamase enzyme inactivity, the carboxylic acid should be deprotected in monomer **1** and incubated with the enzyme for further analysis. Deprotecting monomer **1** may also allow the substrate to dissolve in water as well as enabling β-lactamase activity. With the lack of β-lactamase enzyme activity on substrate monomer **1**, the deprotection of the carboxylic acid is the most sensible step.

4.4 – Conclusions

In the presence of phosphoric acid, polymers $\mathbf{5_F}$ and $\mathbf{5_R}$ have shown carbamate cleavage of PEG by mass spectrometry in entries 1-6. However, this may be a false positive as a result of the ionization at the weak carbamate bond. The self-assembly of micellar nanoparticles can only be confirmed in entry 2 by TEM. Entry 3 displays polymer aggregates, however the material is not well defined. TEM images of entries 1 and 4 do not provide convincing evidence for particle formation. Entry 5 and 6 should be analyzed by TEM along with the appropriate controls.

Ultimately, the assembly of these β-lactamase-responsive polymeric materials has shown some promising results in phosphoric acid, however, with respect to enzyme-directed assembly, β-lactamase has not been shown to conclusively cleave substrate monomer **1**. The inability to prove the enzyme cleavage of monomer **1** is also a result of low substrate concentration reactions. At low substrate concentrations, HPLC is limited by its detection capabilities. β-lactamase reactions should be carried out at higher substrate concentrations and analyzed by varying gradients. To define the HPLC concentration detection limit of monomer **1**, various concentration injections of **1** should be analyzed by HPLC to obtain a calibration curve. Obtaining the minimal concentration capable of detection by HPLC of **1** will provide information for the proper β-lactamase reaction conditions. By detecting β-lactamase activity at various substrate concentrations, the K_m of TEM-1 β-lactamase for can be determined for monomer **1**. Furthermore, the t-butyl protected carboxylic acid may be responsible for the lack of β-lactamase accessibility and activity. To address this issue, the carboxylic acid from monomer **1** should be deprotected and further analyzed for β-lactamase hydrolysis. Due to the lack of

detectable β-lactamase activity between both β-lactamase enzymes on monomer **1**, our efforts to form micelle nanostructures were unsuccessful.

4.5. Experimental

4.5.1. General Methods/Instrument Analysis

All reagents were obtained from commercial sources unless otherwise indicated. Penicillinase from *Bacillus cereus* and TEM-1 β-lactamase purchased from Sigma-Adrich and Life Technologies, respectively. Enzyme reactions were monitored by HPLC using a Jupiter 4u Proteo 90A Phenomenex column (150 x 4.60 mm) as described in section **2.7**. Mass spectra was obtained on an Agilent 6230 HR-ESI-TOF MS at the UCSD Chemistry and Biochemistry Department Molecular Mass Spectrometry Facility. TEM Images were acquired on a formvar carbon grid (Ted Pella, INC.) with 1% uranyl acetate stain on a FEI Technai G2 Sphera at 200 KV.

4.5.2 – Acid Hydrolysis Control

Polymers $\mathbf{5_F}$ (199.09μM) and $\mathbf{5_R}$ (126.74μM) dissolved in methanol were prepared for phosphoric acid hydrolysis analysis before dialysis. A 50μL solution of $\mathbf{5_F}$ and $\mathbf{5_R}$ in methanol were separately incubated with 100μL phosphoric acid (85% w) in a sonication bath for 3 hours. To the dialyzed polymers, a 50μL solution of $\mathbf{5_F}$ and $\mathbf{5_R}$ (39.23μM) in water were each incubated with 100μL phosphoric acid (85% w) in a sonication bath for 3 hours. Sample injections confirmed the cleavage of polyethylene glycol in all entries ESI-*m/z* 208.20 $[M+H]^+$. Samples were further analyzed by TEM.

4.5.3 – β-lactamase Reactions

Two types of β-lactamase enzymes were examined for substrate cleavage, penicillinase from *Bacillus cereus* and TEM-1 β-lactamase. Penicillinase reactions were carried out in 0.1M Tris•HCl/0.1% BSA pH 7.0 while TEM-1 β-lactamase reactions were carried out in 0.1M PBS pH 7.1. Monomer **1** was prepared in a solution of DMSO (1mM) and diluted in 1 mL of the corresponding reaction buffer. Enzyme reactions were incubated using Denville Scientific Inc. Incublock at 25^{o}C for a minimum of 2 hours. TEM-1 (368.6nM) was added to various concentrations of substrate **1** (1 &10μM) and adjusted to 100μL with PBS buffer solution. Penicillinase (2μM) was also added to various concentrations of substrate **1** (2 & 10μM) and diluted with Tris•HCl buffer solution to final volume of 100μL. The enzyme reaction mixtures were analyzed by HPLC using gradient. Peaks were collected and analyzed by ESI-MS.

4.6 – References

(1) Dreher, M. R.; Simnick, A. J.; Fischer, K.; Smith, R. J.; Patel, A.; Schmidt, M.; Chilkoti, A. *J Am Chem Soc FIELD Full Journal Title:Journal of the American Chemical Society* **2008**, *130*, 687-694.

(2) Lee, S. C.; Lee, H. J. *Langmuir* **2007**, *23*, 488-95.

(3) Lee, H. i.; Wu, W.; Oh, J.; Mueller, L.; Sherwood, G.; Peteanu, L.; Kowalewski, T.; Matyjaszewski, K. *Angewandte Chemie International Edition* **2007**, *46*, 2453-2457.

(4) Bhargava, P.; Zheng, J. X.; Li, P.; Quirk, R. P.; Harris, F. W.; Cheng, S. Z. D. *Macromolecules* **2006**, *39*, 4880-4888.

(5) Amir, R. J.; Zhong, S.; Pochan, D. J.; Hawker, C. J. *Journal of the American Chemical Society* **2009**, *131*, 13949-13951.

(6) D'Souza, A. J. M.; Topp, E. M. *Journal of Pharmaceutical Sciences* **2004**, *93*, 1962-1979.